Developmental Biology 453 (2019) 191–205

Contents lists available at ScienceDirect

Developmental Biology

journal homepage: www.elsevier.com/locate/developmentalbiology

Original research article

# GSK3 regulates hair cell fate in the developing mammalian cochlea

Kathryn Ellis [1], Elizabeth C. Driver, Takayuki Okano [2], Abigail Lemons [3], Matthew W. Kelley [*]

*Laboratory of Cochlear Development, National Institute on Deafness and Other Communication Disorders, National Institutes of Health, Bethesda, MD, 20892, USA*

A B S T R A C T

The development of asymmetric patterns along biologically relevant axes is a hallmark of many vertebrate organs or structures. One example is the sensory epithelium of the mammalian auditory system. Two distinct types of mechanosensory hair cells (inner and outer) and at least six types of associated supporting cells are precisely and asymmetrically arrayed along the radial (medial-lateral) axis of the cochlear spiral. Immunolabeling of developing cochleae indicates differential expression of Glycogen synthase kinase 3β (GSK3β) along the same axis. To determine whether GSK3β plays a role in specification of cell fates along the medial-lateral axis, GSK3 activity was blocked pharmacologically in cochlear explants. Results indicate significant changes in both the number of hair cells and in the specification of hair cell phenotypes. The overall number of inner hair cells increased as a result of both a shift in the medial boundary between sensory and non-sensory regions of the cochlea and a change in the specification of inner and outer hair cell phenotypes. Previous studies have inhibited GSK3 as a method to examine effects of canonical Wnt signaling. However, quantification of changes in Wnt pathway target genes in GSK3-inhibited cochleae, and treatment with more specific Wnt agonists, indicated that the Wnt pathway is not activated. Instead, expression of *Bmp4* in a population of GSK3β-expressing cells was shown to be down-regulated. Finally, addition of BMP4 to GSK3-inhibited cochleae achieved a partial rescue of the hair cell phenotype. These results demonstrate a role for GSK3β in the specification of cellular identities along the medial-lateral axis of the cochlea and provide evidence for a positive role for GSK3β in the expression of *Bmp4*.

## 1. Introduction

The sensory epithelium of the mammalian cochlea, the organ of Corti (OC), is comprised of a stereotyped mosaic of cells arranged in a highly regular pattern. The proper differentiation and patterning of this mosaic is essential for auditory function; however, our understanding of how this pattern is achieved remains limited (Basch et al., 2016a; Groves and Fekete, 2012). The OC contains two types of innervated mechanosensory hair cells: a single row of afferently innervated inner hair cells (IHCs) and three rows of outer hair cells (OHCs) that are predominantly innervated by efferent neurons, but also receive approximately 5% of the total cochlear afferent innervation (Zhang and Coate, 2017). The IHCs are located on the medial side of the cochlear duct and convert sound stimuli from mechanical forces to neuronal impulses that are carried into the central nervous system via spiral ganglion neurons. The OHCs are located on the lateral side of the OC and cochlear duct and demonstrate electromotility in response to stimulation. This motility acts to modulate overall activity of the cochlear duct in response to sound. Interspersed between each hair cell and between the rows of hair cells are at least six distinct types of supporting cells. In particular, inner pillar cells (IPCs) form a single row that acts to separate the morphologically and functionally distinct medial and lateral domains (Driver and Kelley, 2009; Kelley et al., 2009).

In the mouse, the cells that give rise to the OC are thought to initially develop as a prosensory domain within the cochlear duct. Prosensory cells become post-mitotic in an apical-to-basal gradient that initiates on embryonic day 12 (E12) and is completed by E14 (Chen and Segil, 1999; Ruben, 1967). At this stage in development, the prosensory domain appears as a homogenous group of morphologically indistinguishable cells. However, over the next few days, these cells undergo rapid differentiation and reorganization to give rise to medial and lateral domains, each of which contains unique types of hair cells and supporting cells. While many of the genes and pathways responsible for the specification of the sensory epithelium (*Sox2*, *Fgf20*, Notch, Hedgehog) (Basch et al., 2016b; Dabdoub et al., 2008; Driver et al., 2008; Hartman et al., 2010; Hayashi et al., 2008; Kiernan et al., 2005a) and hair cells (*Atoh1*) (Bermingham et al., 1999; Woods et al., 2004; Zheng and Gao, 2000) have been identified, our understanding of the factors that partition the prosensory region into functionally distinct medial and lateral domains is comparatively limited (Basch et al., 2016a; Deng et al., 2014; Gu et al., 2016; Munnamalai and Fekete, 2016; Pan et al., 2012).

Glycogen synthase kinase 3 (GSK3) is a serine-threonine kinase,

* Corresponding author. Porter Neuroscience Research Center, 35 Convent Dr., Bethesda, MD, 20892, USA.
*E-mail address:* kelleymt@nidcd.nih.gov (M.W. Kelley).
[1] Current address: Decibel Therapeutics, Boston, Massachusetts.
[2] Current address: Department of Otolaryngology, Heat and Neck Surgery, Graduate School of Medicine, Kyoto University, Kyoto, Japan.
[3] Current address: National Institute on Mental Health, NIH, Bethesda, Maryland.

https://doi.org/10.1016/j.ydbio.2019.06.003
Received 10 January 2019; Received in revised form 7 June 2019; Accepted 7 June 2019
Available online 8 June 2019

originally identified as a modulator of glycogen synthase in response to insulin (Larner et al., 1968). Subsequent studies have demonstrated roles for GSK3 in the modulation of multiple signaling pathways, including canonical Wnt, Hedgehog (Hh), Notch, TGFβ/BMP, and G-protein coupled receptor signaling (Espinosa et al., 2003; Fuentealba et al., 2007; Han et al., 2002; Jin et al., 2009; Patel and Woodgett, 2017; Price and Kalderon, 2002; Tempe et al., 2006). Mammalian genomes contain and express *α* and *β* isoforms of *Gsk3*, which are structurally similar except for differences in their N-terminal domains. In contrast, most invertebrates and birds only express a single *Gsk3* isoform that is most homologous to mammalian *Gsk3β* (Patel and Woodgett, 2017). Knockout studies in mice have shown that *Gsk3α* nulls are viable at birth while *Gsk3β* nulls are embryonic lethal due to liver and heart defects, demonstrating that the more ancestral *Gsk3β* isoform plays a critical role during embryonic development (Hoeflich et al., 2000; Kerkela et al., 2008; MacAulay et al., 2007; Patel et al., 2011). Emerging data suggest that GSK3 modulates diverse aspects of cellular development including proliferation, differentiation, cell fate, migration and cell survival (Kim et al., 2009). However, the role of GSK3 in development of the OC has not been fully explored.

GSK3 is known to play a role in the degradation of β−CATENIN and therefore acts as a negative regulator of the canonical Wnt pathway (Rubinfeld et al., 1996; Stambolic et al., 1996; Yost et al., 1996). In the mammalian cochlea, activation of canonical Wnt signaling leads to an increase in the number of cells that develop as hair cells, as well as an increase in proliferation of the cells in the prosensory domain (Jacques et al., 2012; Munnamalai and Fekete, 2016; Roccio et al., 2015). Moreover, inhibition of GSK3 in the cochlea using high doses of the pharmacological inhibitor CHIR99021 can cause cell cycle re-entry, likely via activation of Wnt signaling (Munnamalai and Fekete, 2016; Roccio et al., 2015). However, given the growing body of work implicating GSK3 in the regulation of other signaling pathways, and the significant phenotypic effects of activation of canonical Wnt signaling, we wanted to examine potential additional roles of GSK3 that might be mediated through non-Wnt pathways by using lower doses of GSK3 antagonists. Our results confirm roles for GSK3 in patterning along the medial-lateral axis of the OC, but in contrast with previous studies (Jacques et al., 2014; Munnamalai and Fekete, 2016; Roccio et al., 2015), we demonstrate that at least some of these effects are not mediated through canonical Wnt signaling. In particular, we show that *Bmp4*, which is expressed in cells located lateral to the OHC region of the OC (Ohyama et al., 2010), is positively regulated by GSK3, and that some of the effects of GSK3 inhibition can be rescued through the addition of BMP4 protein.

## 2. Results

### 2.1. GSK3β is expressed in the lateral domain of the developing cochlea

The OC is comprised of a rigorous mosaic of sensory hair cells (HCs) and non-sensory supporting cells (SCs) that extends along the long axis of the cochlear spiral. In cross-section, two morphologically distinct domains are present (Fig. 1). The medial quarter contains a single row of IHCs surrounded by inner phalangeal cells, while the lateral three-quarters contain three rows of OHCs similarly surrounded by Deiters' cells. As discussed, the innervation patterns and functions of IHCs and OHCs are fundamentally different. Similarly, inner phalangeal cells make contiguous contacts with neighboring IHCs, while Deiters' cells only contact OHCs at the extreme basal and lumenal ends. The medial and lateral regions are separated by two rows of pillar cells, which form the tunnel of Corti. Finally, Hensen's cells and Claudius cells are located directly adjacent to the lateral side of the OHC region, forming a boundary between sensory and non-sensory regions of the OC.

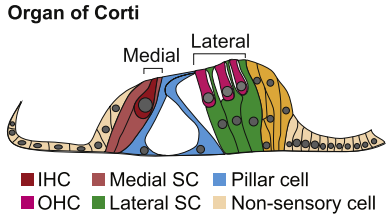


**Fig. 1. Anatomy of the organ of Corti**
Schematic cross-section through the organ of Corti from an adult mouse. Two separate hair cell-containing regions, medial and lateral, are separated by two rows of pillar cells. The medial region contains inner hair cells, inner phalangeal cells, and border cells, while the lateral region contains outer hair cells and Deiters' cells.

To examine the expression of GSK3β, immunohistochemistry using an anti-GSK3β antibody (Miyashita et al., 2009) was performed at various stages of cochlear development (Fig. 2). Because the cochlea develops in a gradient that extends from base to apex, analysis was restricted to the basal region at each time point. Relative cochlear development in more apical regions trails the base by approximately 24 h in the middle region and 48 h in the apex. So, the developmental stages illustrated for the base of the cochlea in Fig. 2 would be present in the middle and apical regions 1–2 days later. At E14.5, GSK3β is expressed in a single row of cells located near the medio-lateral boundary of the OC, but lateral to the developing IHCs. Previous studies have demonstrated that this position corresponds with the location of developing inner pillar cells (IPCs) (Driver et al., 2017; Jacques et al., 2007; Mansour et al., 2009; Mueller et al., 2002; Shim et al., 2005). Expression of GSK3β is considerably lower in the developing OHC region but is broadly expressed in cells lateral to the sensory epithelium including developing Hensen's and Claudius cells (Fig. 2A and B). At E16.5 medial expression of GSK3β persists in IPCs with somewhat weaker expression also present in outer pillar cells (OPCs), inner phalangeal cells (IPhCs), and border cells. Lateral expression in Hensen's and Claudius cells persists (Fig. 2C and D). At birth (P0), overall expression of GSK3β is markedly decreased, but GSK3β is still detectable in IPCs and Hensen's and Claudius cells (Fig. 2E and F). Specificity of GSK3β expression was confirmed using a second anti-GSK3β antibody (Wang et al., 2013) from a different vendor which produced the same results (data not shown, see methods for more details). No expression of GSK3α was detected in the developing cochlea at any of the time points analyzed (not shown).

### 2.2. GSK3 inhibition leads to an increase in IHCs and decrease in OHCs

To examine the role of GSK3β in cochlear development we used two pharmacological inhibitors of GSK3 (both α and β forms) in cochlear explants, CHIR99021 and BIO-acetoxime (Bennett et al., 2002; Spokoini et al., 2010). While both inhibitors showed the same phenotype, we used CHIR9901 for the duration of the study because it has been shown to be the most specific inhibitor of GSK3 and to have lower levels of cytotoxicity relative to BIO-acetoxime (Kramer et al., 2012; Naujok et al., 2014). Explants were established at E13.5, after much of the prosensory domain has exited the cell cycle, but before cellular differentiation. Cochlear explants were treated with either 2 μM CHIR99021 (hereafter referred to as CHIR) or a comparable concentration of DMSO for 4–6 days in vitro (E17.5 to P0 equivalent), at which point explants were fixed and processed for imaging. Culture media containing pharmacological inhibitor or vehicle was changed every day. A dose of 2 μM was determined to be the lowest dose that elicited any phenotypic change in the epithelium. This dose is > 300-fold above an $IC_{50}$ value that was determined using an in vitro enzymatic assay (Ring et al., 2003), but is consistent with previous in vitro studies in which CHIR was shown to block the activity of GSK3 at concentrations between 3 and 10 μM (Jacques et al., 2012; Munnamalai and Fekete, 2016; Roccio et al., 2015). BIO-acetoxime, which has an $IC_{50}$ value of 10 nM in enzymatic assays (Meijer et al., 2003) was used at a concentration of 1 μM based on similar previous results (Jacques et al., 2012; Munnamalai and Fekete, 2016).

Inhibition of GSK3β using either CHIR or BIO-acetoxime caused a

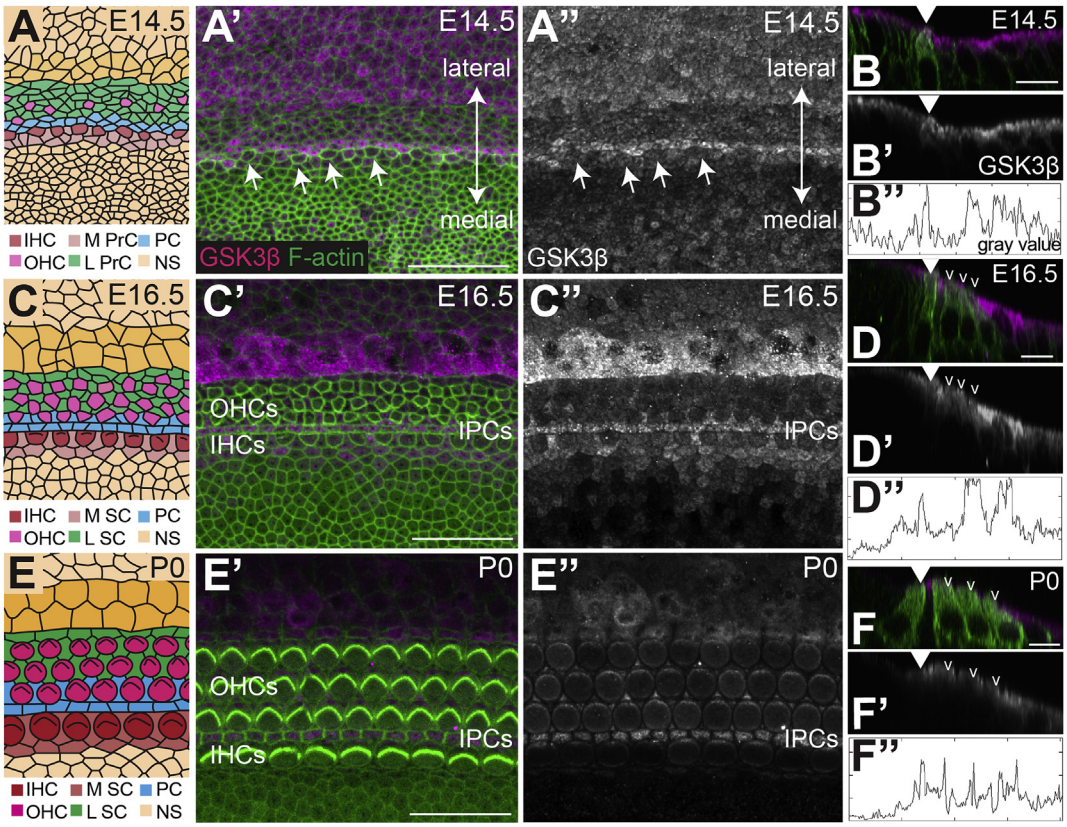


**Fig. 2. GSK3β is expressed in the developing cochlea**

**A, C, E.** Cartoon images of the surface of the cochlea in the basal region at the indicated time points. See A′ for orientation. Cells are colored based on identity. Abbreviations: IHC: inner hair cell, OHC: outer hair cell, M PrC: medial prosensory cell, L PrC: lateral prosensory cell, IPC: inner pillar cell, NS: non-sensory cell, M SC: medial supporting cell, L SC: lateral supporting cell. **A'**. Confocal images of the basal region of the cochlea at E14.5 labeled with anti-GSK3β (magenta) and F-actin by phalloidin (green). **A''**. GSK3β channel alone. GSK3β is expressed in a stripe of cells located just lateral to the developing IHCs (arrows). The cells located in this position will develop as IPCs. Similar levels of GSK3β are also present in cells located lateral to the sensory epithelium. These cells will develop as Hensen's and Claudius cells and the outer sulcus. **B, B'**. Orthogonal views of GSK3β expression at E14.5. In B, the medial border of the prosensory domain is marked by a developing inner hair cell (anti-MYO7A in green, arrowhead). **B''**. Fluorescence intensity profile for GSK3β expression at the apical surface of the epithelium. X-axis for the graph corresponds with position along the medial-to-lateral axis in **B**. Notice that peak intensity corresponds to the IPCs and Hensen's/Claudius/outer sulcus cells. **C′, C''**. At E16.5 GSK3β is expressed in the IPCs, OPCs, IPhCs, and border cells and more intensely in a restricted group of cells lateral to the sensory epithelium. **D, D'**. Orthogonal views of GSK3β expression in magenta and grayscale at E16.5. MYO7A labels inner (closed arrowhead) and outer (open arrowheads) hair cells in green. **D''**. Fluorescence intensity plot profiles of GSK3β expression. Intensity line drawn across apical surface of cells. Notice the peaks of intensity corresponding to the IPCs and Hensen's/Claudius cells. **E, E'**. At P0 overall expression of GSK3β appears reduced but can still be detected in IPCs and Hensen's and Claudius cells. **F, F'**. Orthogonal views of GSK3β expression in magenta and grayscale at P0. **F''**. Fluorescence intensity plot profiles of GSK3β expression. Intensity line drawn across apical surface of cells. Scale bars (A, C, E) = 25 μm. Scale bars (B, D, F) = 10 μm.

dramatic shift in the number of hair cells that developed in the medial and lateral domains of the OC (Fig. 3A–C). As described previously, in control cochlear explants the sensory epithelium develops largely normally, and patterning is almost identical to that observed *in vivo*, including a single row of IHCs and 3–4 rows of OHCs (Driver and Kelley, 2010). However, an additional row of IHCs and several additional rows of OHCs are often observed in the apical third of some control explants, most likely because of defects in cochlear outgrowth that occur because of the explanting process (Driver and Kelley, 2010). In contrast with DMSO-treated controls, explants treated with a GSK3 inhibitor showed a dramatic increase in the number of IHCs, and a roughly comparable decrease in the number of OHCs (Fig. 3A and B). To quantify this result, the total number of IHCs and OHCs was determined for control or CHIR-treated explants. Results confirmed a significant increase in IHCs and a significant decrease in OHCs, as well as a significant increase in the total number of hair cells (IHCs + OHCs) in GSK3-inhibited explants due to the development of supernumerary IHCs (Fig. 3F). While the changes in hair-cell-type distribution were observed along the length of cochlear explants, the effect of GSK3-inhibition was more severe in the apex, where almost all hair cells developed as IHCs (arrows, Fig. 3B and C). This result suggests that the effects of GSK3 inhibition are dependent on developmental timing. To examine this result further, explants were established at E13.5 but not treated with GSK3 inhibitor until E16.5 (Fig. 4A-B'). Results indicated no shift in medio-lateral hair cell fates in these explants, consistent with a limited developmental period during which GSK3β can influence the fates of cochlear prosensory cells (Fritzsch et al., 2006).

To determine whether the change in hair cell locations relative to the medial-lateral boundary represented an actual change in cell fate, the experiments described above were repeated using cochlear explants from *Fgf8*$^{GFP}$ transgenic mice that express GFP specifically in IHCs (see Methods). Results confirmed that the additional medial HCs present in CHIR-treated explants are positive for *Fgf8*$^{GFP}$, indicating that they are IHCs (Fig. 3D-E) Consistent with the *Fgf8*-reporter results, all medial hair cells in CHIR-treated explants are also positive for S100A1, which labels IHCs and Deiters' cells (Coppens et al., 2001; Woods et al., 2004), N-cadherin, expressed by medial IHCs and SCs (Chacon-Heszele et al., 2012)), and higher levels of Calbindin relative to the OHCs (Dechesne and Thomasset, 1988), further confirming that the extra medial HCs in CHIR-treated explants are specified as IHCs (Fig. 3G-L).

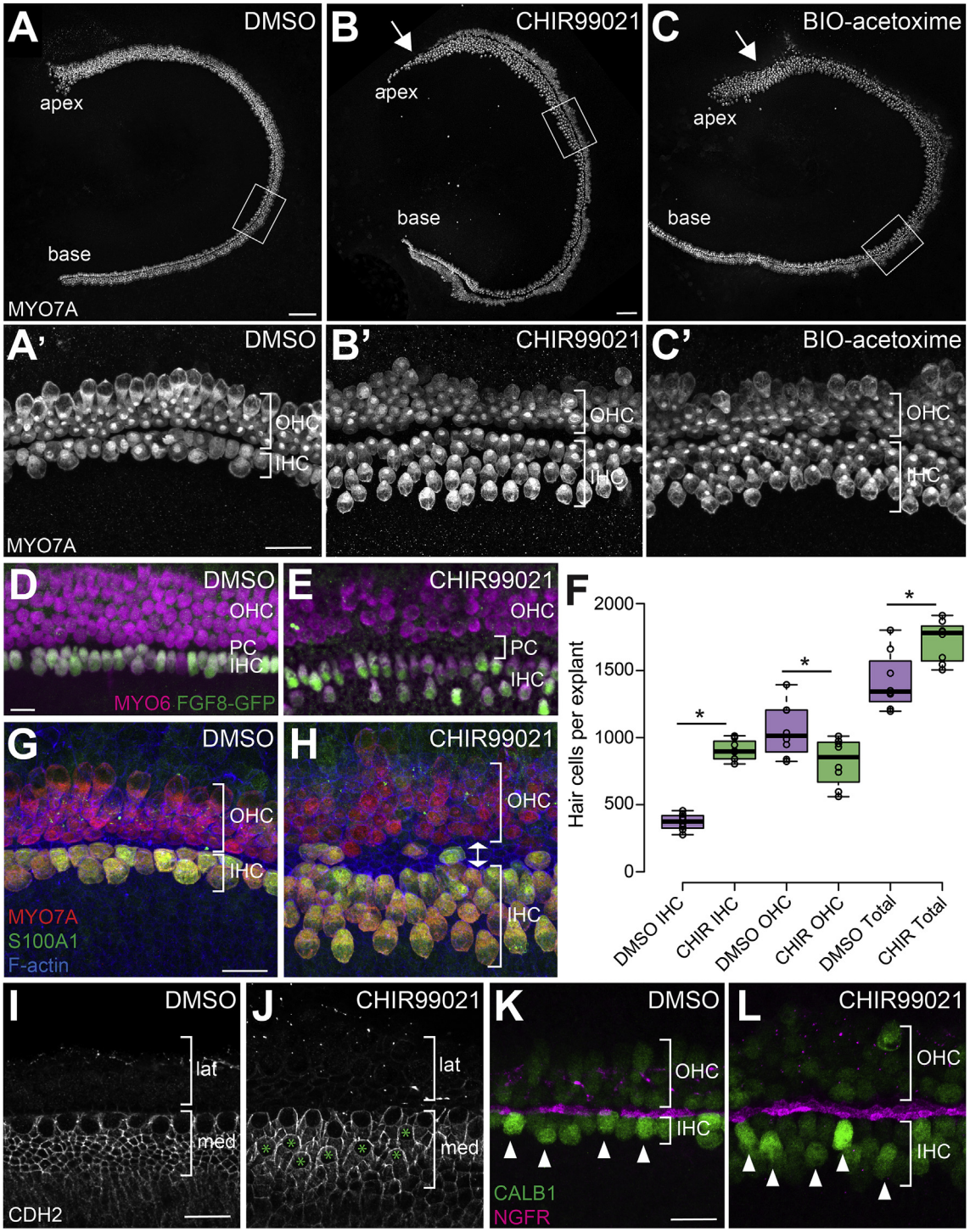


**Fig. 3. Inhibition of GSK3 leads to an increase in IHCs and a decrease in OHCs**

**A-C.** Inhibition of GSK3 in cochlear explants using 2 μM CHIR99021 (B) or 1 μM BIO-acetoxime (C) results in an increase in the number of IHCs and a decrease in the number of OHCs compared to DMSO-treated controls (A). Hair cells are labeled with anti-MYO7A. **A′-C′**. Magnified view of hair cells in the middle region of explants (boxed regions in **A-C**) illustrating the difference in IHC and OHC numbers between control and GSK3-inhibited samples. Note the significant increase in the number of IHCs and the relative decrease in OHCs. **D-E.** Magnified view of explants from *Fgf8*$^{GFP}$ cochlea showing that extra IHCs in GSK3-inhibited cochleae are positive for *Fgf8*. All hair cells labeled with anti-MYO6 in magenta. IHCs labeled with anti-GFP (*Fgf8*) in green. Bracket in **E** indicates the increased PC region (increased distance between rows of IHCs and OHCs). **F.** Quantification of the change in number of IHCs, OHCs, and total HCs as a result of inhibition of GSK3. DMSO-treated control explants N = 8. CHIR-treated explants N = 8. Difference in IHCs $p < 0.0001$. Difference in OHCs $p = 0.025$. Difference in total hair cells $p = 0.007$. **G, H.** Labeling with anti-S100A1 (green), which marks IHCs and Deiters' cells, confirms extra hair cells on medial side are specified as IHCs. Double arrow in **H** shows extra width of PC region in CHIR-treated explants. **I, J.** Anti-N-cadherin (CDH2) staining is found in the medial (med) but not lateral (lat) domain of DMSO (**I**) and CHIR-treated **(J)** explants. Extra IHCs (green asterisks in **J**) and surrounding SCs are CDH2-positive. **K, L.** Anti-Calbindin (CALB1, green) staining is brighter in both endogenous and supernumery IHCs (arrowheads), relative to OHCs. IHCs and OHCs are separated by IPCs stained by anti-NGFR (magenta). Scale bars (A–C) = 100 μm. Scale bars (A′–C′) = 25 μm. Scale bars (D–L) = 20 μm.

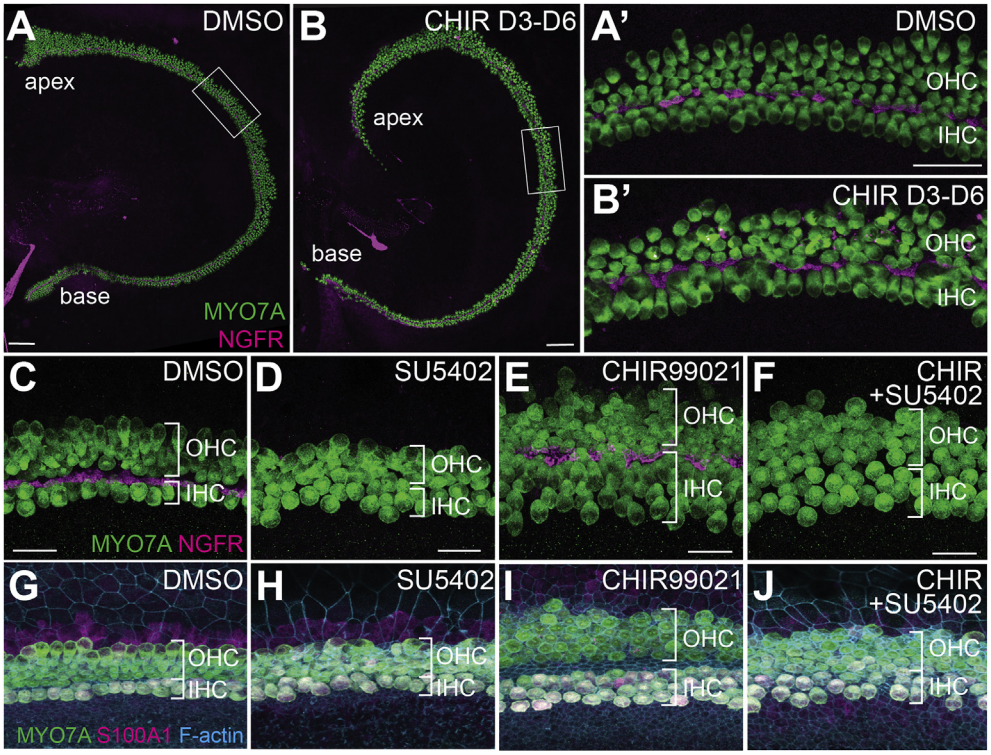


**Fig. 4. Effects of GSK3 inhibition are dependent on developmental stage, and its effects on inner pillar cells are dependent on activation of FGFR**

**A, A**'. DMSO-treated explants have the expected 1:3 ratio of IHC to OHC. Hair cells are labeled with anti-MYO7A (green), IPCs are labeled with anti-NGFR (magenta). **B, B**'. Explants established at E13.5 but not treated with CHIR until E16.5 (3 days of CHIR-treatment total) show no change in the ratio of IHC:OHC. Position of regions shown in **A**′, **B**′ are indicated by boxes in **A** and **B. C-J.** Increase in number of pillar cells in CHIR-treated explants is mediated through Fgfr. **C,G.** DMSO-treated control explants labeled with anti-MYO7A (green) and anti-NGFR (magenta) in C to illustrate hair cells and pillar cells or with anti-MYO7A (green) and anti-S100A1 (magenta) to label inner hair cells (G). **D,H.** Treatment with the Fgfr-antagonist SU5402 (10 μM) results in loss of IPCs as previously reported. **E,I.** GSK3-inhibition results in an increase in the number of IHCs and IPCs. **F,J.** Treatment with both CHIR and SU5402 results in a loss of the supernumerary IPCs, but extra IHCs are still present. Scale bars (A, B) = 100 μm. Scale bars (A′, B′) = 50 μm. Scale bars (C–F) = 20 μm.

In many GSK3-inhibited explants we also noted an increase in the number of IPCs, demonstrated by an expansion of labeling with the IPC marker NGFR (formerly p75) and in increase in distance between the IHCs and OHCs (Fig. 3A–H). IPC development is regulated through expression of *Fgf8* in IHCs (Jacques et al., 2007; Mueller et al., 2002), suggesting that the increased IPCs might be a result of increased Fgf8 availability in GSK3-inhibited explants. To determine whether this is the case, explants were treated with both CHIR and the Fgfr antagonist SU5402. Double-treated explants had a persistent increase in the number of IHCs, but a complete absence of IPCs (Fig. 4C–J). This finding is consistent with an indirect effect of GSK3-inhibition on IPC development through an increase in the number of IHCs.

### 2.3. GSK3 inhibition causes an expansion of the sensory epithelium

Inhibition of GSK3 led to an increase in the overall number of hair cells (Fig. 3F). Therefore, we sought to determine if CHIR-treatment caused an increase in the size of the prosensory domain, which could then lead to increased hair cells in the OC. To examine this possibility, explants were established at E13.5, treated with CHIR for 48 h in vitro (E15.5 equivalent), and then fixed. Anti-SOX2 was used to visualize the prosensory domain. Results indicated an expansion in the size of the sensory epithelium in explants treated with CHIR, as compared to controls (Fig. 5A,B,E). This expansion was especially pronounced in the medial domain of the OC. Since SOX2 is initially broadly expressed in the entire medial half of the cochlea duct before becoming restricted to the prosensory domain (Gu et al., 2016; Kiernan et al., 2005b), increased medial expression in the OC in CHIR-treated explants was most likely a result of persistent expression in this region. In contrast with the observed changes in width, inhibition of GSK3 did not lead to a significant increase in the length of the prosensory domain (Fig. 5F). To determine whether the increased prosensory domain lead to a direct increase in the number of cells that develop as hair cells, explants from transgenic *Atoh1*$^{GFP}$ mice were established. In CHIR-treated explants, there were significantly more GFP-positive hair cells at E15.5 equivalent, as compared to controls. Consistent with the results observed at E17.5 equivalent, the extra hair cells were located in the medial domain (Fig. 5C, D, G).

To determine whether the expansion of the SOX2 positive prosensory domain occurred because of increased proliferation, explants were established at E13.5 and treated with CHIR in the presence of EdU for 24 h. At E14.5, the EdU was washed out and the explants were maintained for an additional 24 h with continued CHIR-treatment. Results indicated no significant difference in the number of SOX2 and EdU double positive cells in GSK3-inhibited explants and controls (Fig. 5H, I, L). The few double positive nuclei that were observed were predominantly found in the lateral domain, even though expansion of the SOX2 domain was predominantly localized to the medial domain (Fig. 5J and K). This result contrasts with previous studies of GSK3 inhibition in the cochlea which reported significant increases in proliferation in the lateral domain. This difference is most likely a result of difference in dosage of CHIR (see Discussion).

Taken together, these data suggest that inhibition of GSK3 leads to a change in the position of the medial boundary of the OC, such that cells located medial to the OC, which would nornally develop as non-sensory cells, instead develop as part of the OC. One effect of this expansion is the formation of supernumerary IHCs.

### 2.4. The medio-lateral boundary of the OC is disrupted in GSK3-inhibited explants

While the altered position of the medial boundary of the OC in response to inhibition of GSK3 could account for some or all of the increase in number of IHCs, the size of the lateral domain appeared unchanged (based on expression of SOX2), despite a significant decrease in the number of OHCs. To determine whether this was the case, explants were labeled with an antibody against PROX1, a marker of the lateral domain (Bermingham-McDonogh et al., 2006). Quantification indicated no significant change ($p = 0.658$) in the number of PROX1-positive cells in control (average number of PROX1 positive hair cells = 851± 59. N = 5 explants) and CHIR-treated explants (912 ± 116, N = 5) in a 750 μm stretch in the middle region (Fig. 6A-B′). This result suggested

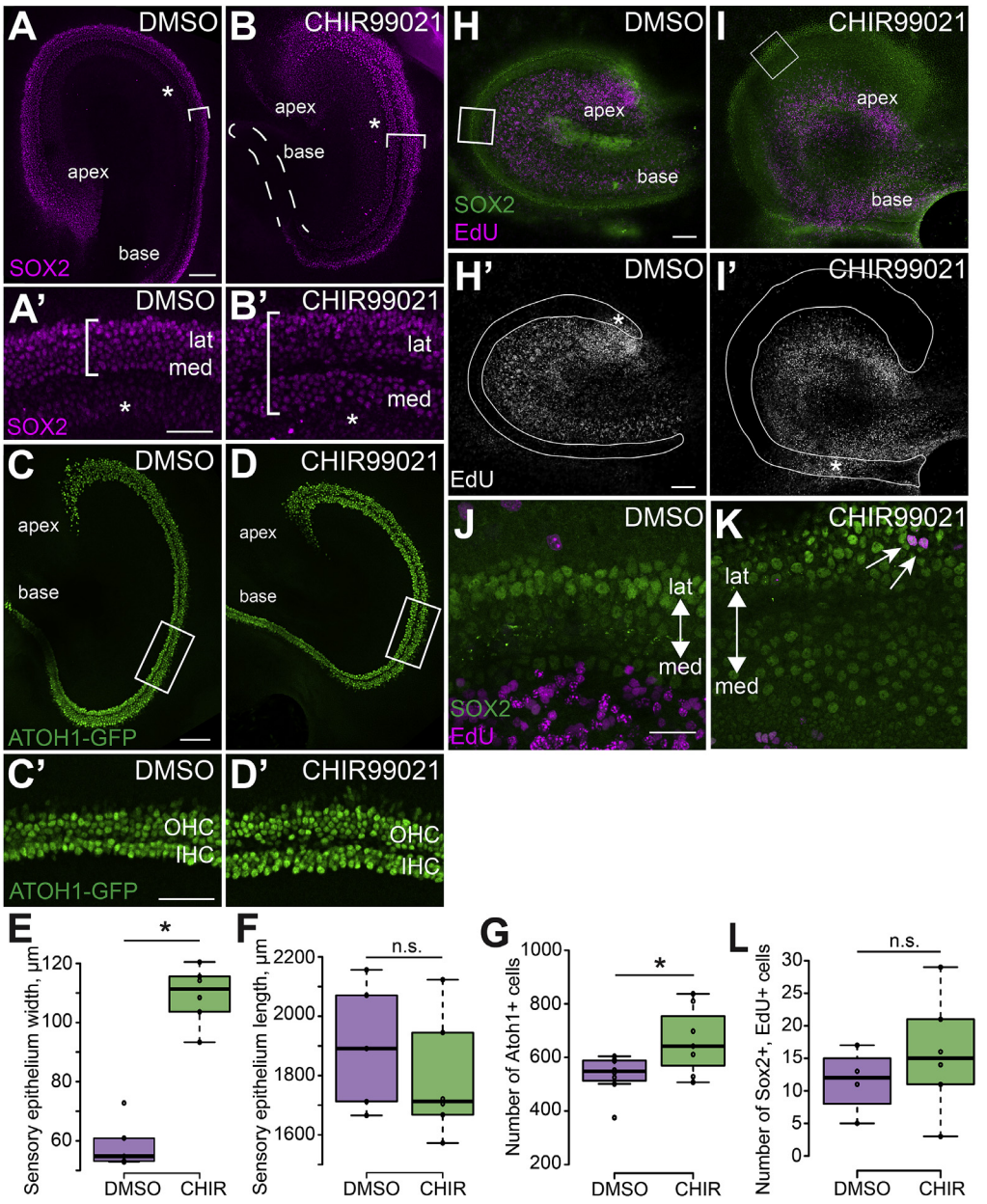


**Fig. 5. Inhibition of GSK3 causes an increase in the size of the prosensory domain but does not increase cell proliferation**

**A, B.** Cochlear explants established at E13.5 and fixed at E15.5. Labeling with anti-SOX2 (magenta) illustrates the increased size of the prosensory domain (brackets) in explants treated with CHIR (B) as compared to controls (A). This expansion is especially pronounced in the medial domain. Asterisks label low level expression of SOX2 in Kölliker's organ. Dashed line in **B** outlines the basal prosensory region. **A′, B**'. High magnification images of the middle regions from the explants in A and B showing the expanded medial domain. The width of the SOX2 positive prosensory domain is indicated by the brackets. Asterisks label low level expression of SOX2 in Kölliker's Organ. **C, D.** Expression of *Atoh1*$^{GFP}$ indicates increased initial formation of hair cells in explants treated with CHIR (D) as compared to DMSO-treated controls (C). **C′, D**'. High magnification views of the boxed regions in C and D illustrating increased *Atoh1*$^{GFP+}$ IHCs in an explant treated with CHIR. Note that these images are rotated 90° relative to the images in C and D. **E, F.** Quantification of sensory epithelium width (measured at the mid-point of each explant) and overall length in explants established at E13.5 and fixed at E15.5. CHIR-treatment leads to a significant increase in the width of the developing sensory epithelium while the length remains unchanged. DMSO-treated explants N = 5. CHIR-treated explants N = 6. Width $p < 0.0001$. Length $p = 0.411$. **(G)** Quantification of average number of *Atoh1*$^{GFP+}$ hair cells counted in a 750 µm stretch in the middle region of DMSO-treated explants (N = 8) and CHIR-treated explants (N = 7). *Atoh1*$^{GFP+}$ hair cells are significantly increased following CHIR-treatment. $p = 0.045$. **H – K.** Cochlear explants were established at E13.5 and treated with EdU for 24 h from E13.5 – E14.5. Explants were maintained in medium containing DMSO or CHIR for an additional 24 h and then fixed. EdU-positive nuclei (magenta) in the sensory epithelium were identified based on co-expression of SOX2 (green) in DMSO-treated control (H) and CHIR-treated explants (I). Note that there is minimal overlap between EdU$^{+}$ cells and Sox2$^{+}$ cells. **H′, I**'. The same images as in H and I but showing only the EdU labeling. The sensory epithelium is outlined based on expression of SOX2. Asterisks indicate proliferating mesenchymal cells located below the basement membrane of the sensory epithelium. Mesenchymal proliferation was consistently seen across all cultures. **J, K.** Magnified view of the middle regions of control (J) and CHIR-treated (K) cochlear explants (boxed regions in H and I) showing a few cells that are co-labeled with SO×2 and EdU. Arrows indicate SOX2 and EdU double positive cells. Double-positive cells were almost always found in the lateral domain. Note that these images are rotated relative to the images in H and I. **L.** Quantification of SOX2 and EdU double-positive cells. DMSO and EdU treated explants N = 4. CHIR and EdU treated explants N = 6. Difference between DMSO and CHIR explants double positive cells $p = 0.371$. Scale bars (A, B, C, D, H, I) = 100 µm. Scale bars (A′, B′) = 50 µm. Scale bars (J, K) = 25 µm.

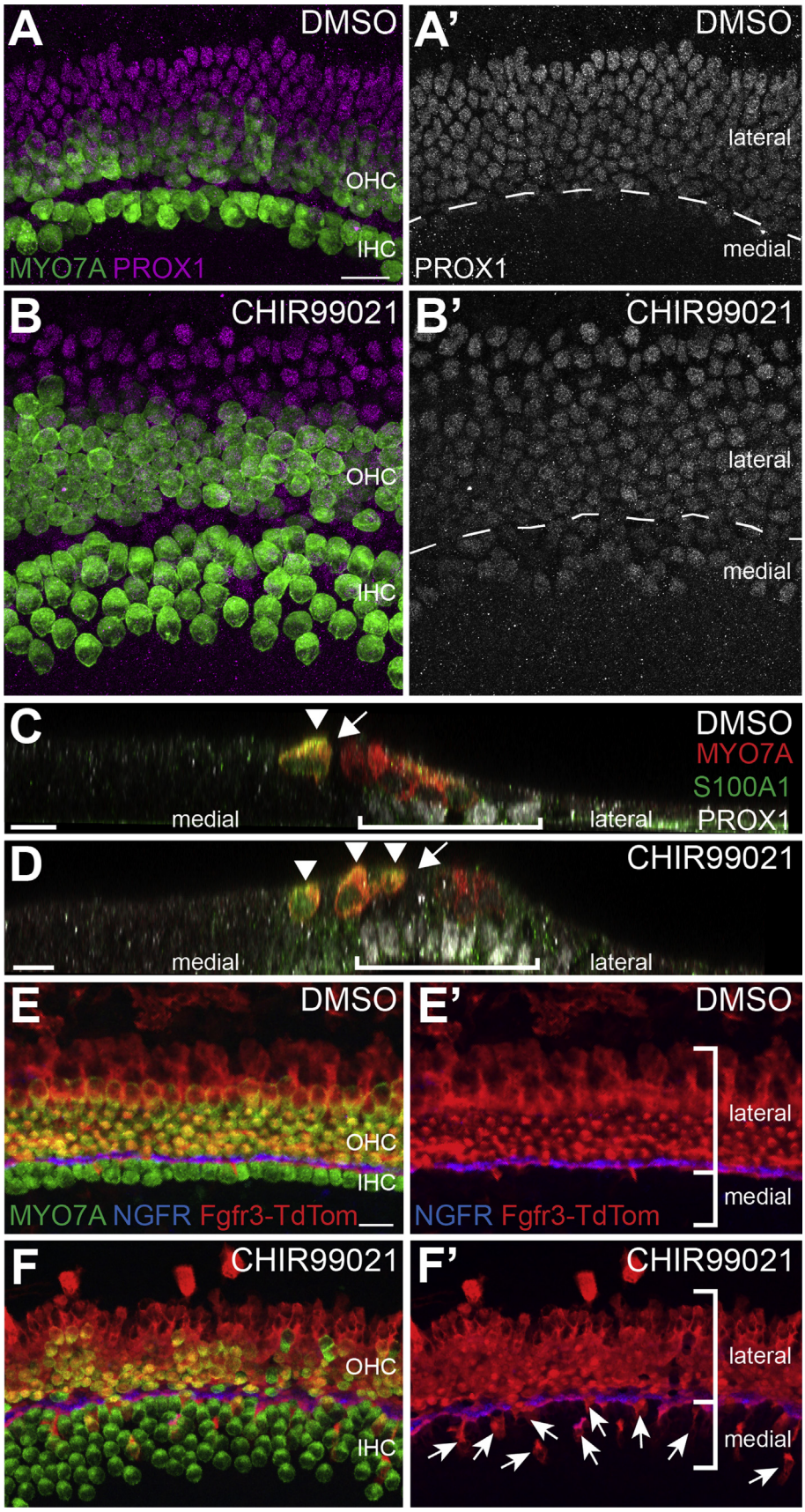


**Fig. 6. Disruption of the medio-lateral boundary in GSK3-inhibited explants is partly due to lateral cells adopting medial cell fates**

**A, B.** Control (**A, A'**) and CHIR-treated (**B, B'**) explants labeled with anti-MYO7A (green) and anti-PROX1 (magenta). In DMSO-treated controls the boundary of PROX1 aligns precisely with the row of IPCs (dashed line in **A'**). In contrast, in CHIR-treated explants, PROX1 expression extends into the medial domain (below dashed line in **B'**). **C, D.** Confocal orthogonal views of the sensory epithelium from control (C) or CHIR-treated explants (D). Hair cells are labeled in red (MYO7A) and PROX1$^{+}$ supporting cells are in white. S100A1 in green indicates IHCs and Deiters' cells. In the control, PROX1$^{+}$ cells (bracket) are located lateral to the pillar cells (arrow). In contrast, in the CHIR-treated explant PROX1$^{+}$ supporting cells are present beneath extra IHCs (**D**, arrowheads). Pillar cells are indicated with an arrow. **E-F'**. Cochlear explants from transgenic *Fgfr3*$^{creErt2}$;*R26R*$^{TdTom}$ mice were established at E13.5 and maintained in either DMSO or CHIR from E13.5 – E17.5. Explants were treated with 1 μM 4-OH-Tamoxifen from E13.5 – E15.5 to induce recombination. **E, E'**. In controls, *Fgfr3*$^{creErt2}$;*R26R*$^{TdTom}$ positive cells (red) are largely restricted to the lateral domain. Hair cells are labeled with MYO7A (green) and IPCs are labeled with NGFR (blue). (**F, F'**) Inhibition of GSK3 causes a significantly increased number of lateral, *Fgfr3*$^{creErt2}$;*R26R*$^{TdTom}$ positive cells to adopt medial IHC, inner phalangeal cell, or border cell fates. Labeling as in E. Arrows indicate medial cells that are tdTomato-positive. Scale bars = 20 μm.

that the decrease in OHCs was a result of either a decrease in the number of HCs that form in the lateral domain, or a change in the position of the boundary between the medial and lateral domains. To discriminate between these possibilities, PROX1 labeling was combined with MYO7A labeling to identify the medial-lateral boundary. In control explants, the domain of PROX1 expression correlated precisely with the lateral boundary extending from the IPCs to the Hensen's and Claudius cells (Fig. 6A). In contrast, in GSK3-inhibited explants PROX1 expression extended past the IPC boundary and into the medial IHC domain (Fig. 6B).

To determine whether PROX1-positive supporting cells located in the medial domain undergo a similar change in fate, explants were labeled with anti-S100A1 which labels IHCs as well as lateral Deiters' cells (Woods et al., 2004). Consistent with the results presented in Fig. 2, all medial hair cells in CHIR-treated explants were positive for S100A1, indicating that they were specified as IHCs. Similarly, supporting cells surrounding IHCs in the PROX1 domain were negative for S100A1, indicating that they had not developed as Deiters' cells. In some cases, hair cells were observed within the expanded pillar cell region of CHIR-treated explants. Interestingly, some of these cells were S100A1 positive while others were negative (Fig. 3G and H). This result is consistent with disruption of the medial-lateral boundary in response to inhibition of GSK3.

### 2.5. Fate-mapping confirms a shift in the medial-lateral boundary of the OC in response to inhibition of GSK3

To further test the hypothesis that inhibition of GSK3 leads to a disruption in the medial-lateral boundary, we performed fate mapping using the lateral domain-specific gene *Fgfr3*. First, to confirm the specificity of *Fgfr3* to the lateral domain, *Fgfr3-icreER$^{T2}$; R26R$^{tdTom}$* or *Fgfr3-icreER$^{T2}$; R26R$^{mT\text{-}mG}$* mice were gavaged with 250 μg tamoxifen at E13.5, E14.5, or E15.5 and then maintained until birth. Analysis of cochleae from induced females indicated sporadically recombined cells that were all (788 cells from 31 cochleae) restricted to lateral cell fates (OHC, IPC, OPC or Deiters' cells; data not shown). Next, E13.0 cochlear explants were established from *Fgfr3-icreER$^{T2}$; R26R$^{tdTom}$* mice and then induced at E13.5 for 48 h. Explants were maintained until the equivalent of P0 (6 DIV) before analysis. In contrast with *in vivo* induction, addition of 4-OH-tamoxifen to the media induced much broader recombination resulting in nearly 100% labeling of all cells in the lateral domain (Fig. 6E), In addition, a small number of tdTomato positive IHCs (average of 18 tdTomato-positive IHCs per explant, N = 4 explants) were also observed indicating that, at least *in vitro*, not all *Fgfr3*-positive cells are restricted to lateral fates. It was not possible to determine whether the differing number of *Fgfr3*-derived medial cells *in vivo* and *in vitro* are a result of a culture artifact or of the limited *in vivo* sample size. Next, the effects of inhibition of GSK3 were determined by exposing *Fgfr3-icreER$^{T2}$; R26R$^{tdTom}$* cochlear explants to both 4-OH-tamoxifen and CHIR as described. Results indicated a significantly greater number of *Fgfr3*-positive IHCs (average of 34 tdTomato-positive IHCs per explant, $p = 0.022$, N = 4) following CHIR-treatment. (Fig. 6E and F).

In addition to an increase in the number of *Fgfr3*-positive IHCs, cells surrounding the IHCs, which appear to be IPhCs or border cells, were also positive for *Fgfr3,* although the numbers of these cells were difficult to quantify, as without a marker it is difficult to discriminate IPhCs from adjacent non-sensory cells (Fig. 6F'). Overall, the number of IHCs that were *Fgfr3*-positive, and therefore derived from the lateral domain, was not sufficient to account for either the overall increase in IHCs or for the decrease in OHCs. These results are consistent with the increase in IHCs arising as a result of both changes in specification of HC fates within the normal prosensory domain and a shift in the medial boundary between sensory and non-sensory regions. The fates of *Fgfr3*-positive cells that would have become OHCs in GSK3-inhibited explants is less clear. Many appear to have developed as supporting cells in the lateral domain (Fig. 6F). In particular, as discussed above, there is an increase in IPCs in CHIR-treated explants. As IPCs and OHCs both arise from the same lateral prosensory pool, the increased IPCs may derive from prosensory cells that would have developed as OHCs.

These data, together with the PROX1 data, are consistent with a change in the position of the medial-lateral boundary in response to inhibition of GSK3, leading to laterally fated cells switching fates to become IHCs and other medial cell types.

### 2.6. Inhibition of GSK3 does not phenocopy activation of canonical Wnt signaling

As discussed, GSK3 has been shown to stabilize β-CATENIN leading to activation of the canonical Wnt signaling pathway (Patel and Woodgett, 2017). To investigate whether the phenotypes observed in response to treatment with CHIR were a result of activation of canonical Wnt signaling, we compared the effects of GSK3-inhibition with activation of canonical Wnt by treating explants with a Wnt-pathway agonist that directly activates TCF (Liu et al., 2005). In contrast to the large increase in medial cells observed following GSK3-inhibition, direct activation of TCF did not induce a significant change in the number of IHCs compared to DMSO-treated controls (Fig. 7A–D) (Avg. DMSO IHC = 370 ± 10; Avg. WntAg IHC = 317 ± 10). In addition, in contrast to the loss of OHCs seen in explants treated with CHIR, TCF-activation resulted in an increase in the number of OHCs as compared to control (Fig. 7C, Avg. DMSO OHC = 977 ± 43, Avg. WntAg OHC = 1160 ± 56, $p = 0.042$). However, quantification of total number of HCs per explant indicated no significant change in samples treated with WntAg (Fig. 7D) (Avg. DMSO total HC = 1347 ± 46. Avg. WntAg total HC = 1477 ± 66). To determine whether the increase in OHC in WntAg-treated explants was due to a disruption in cochlear convergence and extension, explants from controls and WntAg-treated explants were measured along their long, apical-basal axis. There was no significant difference in the lengths of the two groups (Avg. length of DMSO-treated explants = 1908 ± 63 μm. Avg. length of WntAg-treated explants = 1907 ± 97 μm). Overall, the results indicated significant differences in the phenotypes induced in response to CHIR versus WntAg. These results suggest that the effects of CHIR and, therefore, inhibition of GSK3, are not mediated through the canonical Wnt pathway.

To further investigate whether the phenotypes observed in response to inhibition of GSK3 were mediated through the canonical Wnt pathway, we sought to determine whether the CHIR-mediated changes in the medial-lateral boundary would occur even if the canonical Wnt pathway was inhibited. As a first step, explants were established on E14.5 and treated with 1 μM, 3 μM, or 10 μM of the canonical Wnt/TCF antagonist FH535 (Handeli and Simon, 2008; Liu et al., 2014) for 48 h. Then changes in Wnt target gene expression were assayed by qRT-PCR. Results indicated significant inhibition of the Wnt-targets *Ccnd1* and *Lgr5* in the presence of either 3 or 10 μM FH535 and in *Axin2* at 10 μM FH535 (Fig. 7E). None of the three target genes were significantly increased in response to 2 μM CHIR alone. Next, explants were treated with both 3 μM FH535 and 2 μM CHIR. Wnt target gene expression decreased similarly to treatment with 3 μM FH535 alone, suggesting that treatment with 2 μM CHIR does not significantly activate canonical Wnt signaling. To determine whether changes in the medial-lateral boundary still occur in CHIR-treated explants even when canonical Wnt-signaling is suppressed, explants were established at E14.5 and maintained in DMSO, 2 μM CHIR, 3 μM FH535, or 2 μM CHIR plus 3 μM FH535, for 5 DIV. Development of IHCs and OHCs was then analyzed. As previously reported, inhibition of Wnt signaling led to a significant decrease in the number of hair cells (Jacques et al., 2012; Shi et al., 2014). Moreover, of the HCs that remained, the majority developed as IHCs, presumably because those IHCs remaining were already specified before FH535 was applied, while the later-developing OHCs were not yet specified. Treatment with the Wnt antagonist FH535 in combination with the GSK3 inhibitor CHIR led to a significant rescue of HCs by comparison with Wnt antagonist FH535 alone, although the total number was still below that

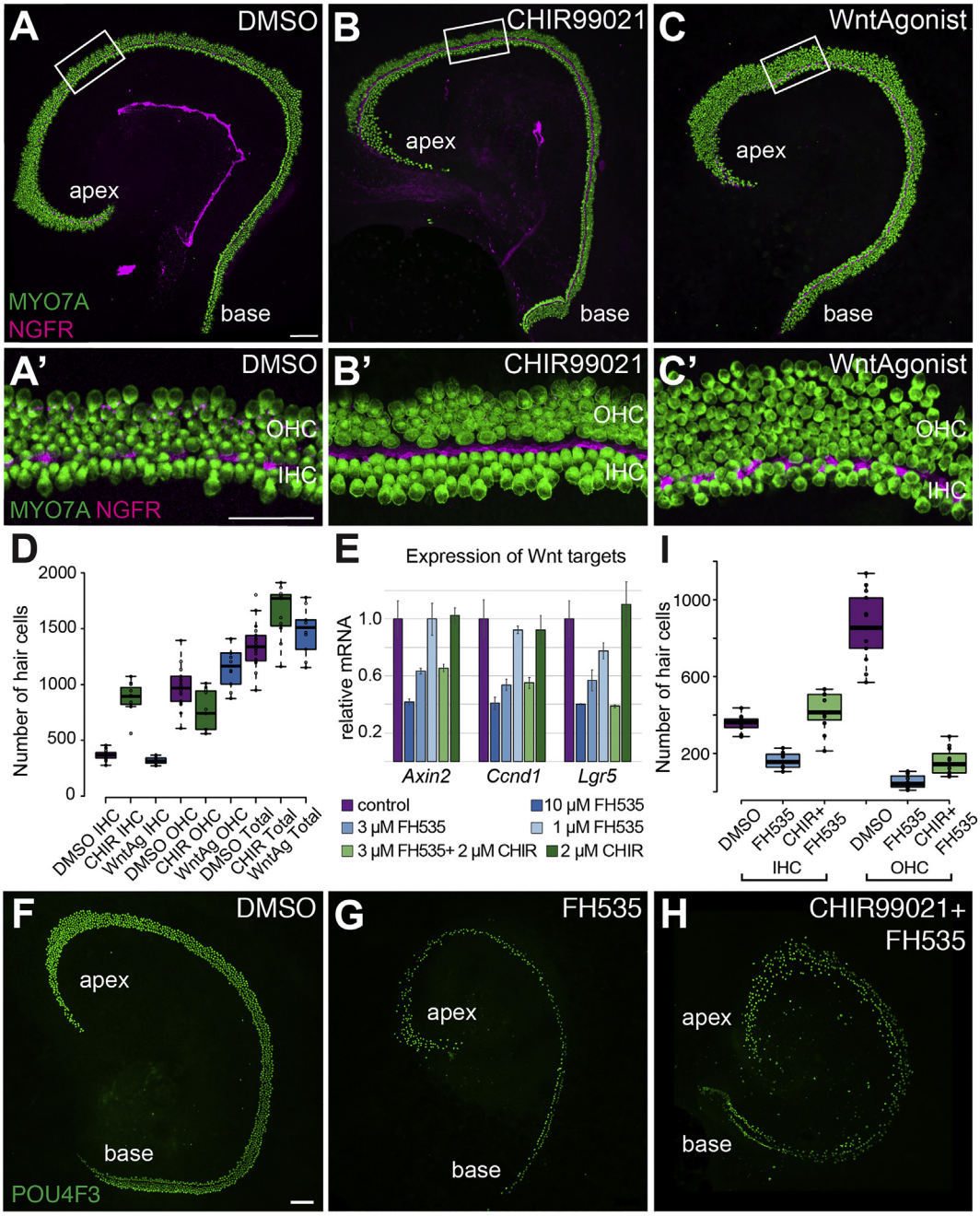


**Fig. 7. Effects of inhibition of GSK3 are not mediated through activation of canonical Wnt signaling**

**A-C**'. Low and high magnification views of Control (A, A′), CHIR-treated (B, B′) or WntAgonist-treated (C, C′) cochlear explants established on E13.5 and maintained under the indicated conditions for 5 DIV. Hair cells are labled with anti-MYO7A (green) and IPCs with anti-NGFR (magenta). In contrast with the effects of treatment with CHIR, treatment with WntAgonist induced an apparent increase in the number of OHCs but has a minimal effect on the number of IHCs (DMSO-treated, N = 18, CHIR-treated, N = 11, WntAgonist-treated, N = 10). **D.** Quantification of hair cell numbers in response to inhibition of GSK3 or activation of canonical Wnt. IHCs and total HCs are significantly increased in CHIR-treated explants while number of OHCs is significantly decreased ($p < 0.0001$, $p = 0.0144$, $p = 0.002$, respectively). In contrast, in explants treated with WntAgonist, the number of IHCs and total hair cells are unchanged by comparison with control (n.s.), but OHCs are increased ($p = 0.042$). Changes in number of IHCs and OHCs but not total HCs were significantly different in WntAgonist-treated cultures by comparison with CHIR-treatment ($p < 0.0001$, $p = 0.0142$, n.s., respectively). **E.** qPCR analysis of changes in Wnt target gene expression in explants treated with CHIR, the Wnt antagonist FH535, or a combination of both at the indicated concentrations. Treatment with increasing concentrations of FH535 induces a dose-dependent inhibition of Wnt-target gene expression. All differences are significant from control for 10 μM FH535, and for 3 μM for *Ccnd1* and *Lgr5*. Addition of CHIR to 3 μM FH535 had no effect on the expression levels of Wnt target genes (no significant differences in values between 3 μM FH535 and 3 μM FH535 + 2 μM CHIR). CHIR alone had no effect on Wnt target gene expression. Data presented as means, ± SEM. **F–H.** Control (F), FH535- (G) or FH535 + CHIR9902-treated (H) explants established at E14.5 and maintained for 5 DIV, stained with anti-POU4F3 to mark HC nuclei. Overall hair cell number is decreased in response to FH535, while addition of CHIR appears to rescue, to some degree, the overall number of hair cells. **I.** Quantification of numbers of IHCs and OHCs in control, FH535, or FH535+CHIR-treated explants. The phenotypic switch in the IHC/OHC ratio that is observed in explants treated with CHIR also occurs when canonical Wnt signaling is inhibited by FH535. All comparisons are significantly different ($p < 0.0001$) except FH535 and FH535 + CHIR OHCs ( n.s.). Scale bars, A-C and F–H, 100 μm, A′-C′, 50 μm.

observed in control. Moreover, there were significantly more IHCs in double-treated explants compared to both controls and FH535 alone-treated ($P < 0.0001$). Analysis of the ratio of IHCs to OHCs showed an increase in the number of IHCs and a decrease in the number of OHCs that was consistent with the phenotypic switch observed in the presence of 2 μM CHIR alone (Fig. 7F–H). These results demonstrated that the changes in HC phenotypes observed in response to inhibition of GSK3 are unlikely to be mediated through the canonical Wnt pathway, since they still occur in the presence of a canonical Wnt antagonist.

### 2.7. BMP4 rescues the effects of GSK3 inhibition in the lateral domain

Since the results of the previous experiments demonstrated that the effects of inhibition of GSK3 were likely not mediated through canonical Wnt signaling, we sought to identify other possible pathways that might regulate the observed changes in HC fates. As described above, the effects of inhibition of GSK3 are most consistent with changes in the locations of boundaries along the medial-to-lateral axis of the cochlear duct. *Bmp4* is expressed in the lateral non-sensory domain of the duct (Morsli et al., 1998; Ohyama et al., 2010) and plays roles in both specification of lateral identities and suppression of medial identities (Ohyama et al., 2010). Since GSK3β is also expressed in the lateral domain of the developing cochlea in a similar pattern to that of *Bmp4* (Fig. 2), we examined the effects of inhibition of GSK3 on expression of *Bmp4* by qPCR. Expression of *Fgf10*, a marker for the medial domain of the cochlear duct (Pauley et al., 2003; Urness et al., 2015) was also examined.

Explants were established as described and treated with DMSO or 2 μM CHIR for 2 DIV. Total mRNA was then extracted and changes in expression of *Bmp4* and *Fgf10* were determined. Explants treated with CHIR showed a significant decrease in expression of *Bmp4* (Fig. 8A, $p = 0.001$). An increase in *Fgf10* was also observed, but the degree of change varied between experiments and, as a result, did not differ significantly from control.

Given the demonstrated role of *Bmp4* in specification of phenotypes along the medial-lateral axis, this result suggested that the effects of inhibition of GSK3 could be mediated, at least in part, through BMP4. To determine whether BMP signaling is affected by GSK3 inhibition, the phosphorylation of a known BMP4-target, SMAD1 (pSMAD1), was examined in explants treated with either 2 μM CHIR or exogenous recombinant BMP4 protein (50 ng/ml). Treatment with BMP4 induced a significant increase in pSMAD1 fluorescence compared to controls (Fig. 8B–E). In contrast, treatment with 2 μM CHIR induced a significant reduction in pSMAD1 fluorescence compared to controls (Fig. 8D and E), confirming that inhibition of GSK leads to a decrease in *Bmp4* expression and activity. Since Bmp4 has been shown to induce lateral fates in the developing organ of Corti (Ohyama et al., 2010), these results suggest that GSK3 might act to induce or maintain *Bmp4* expression in the lateral domain of the cochlear duct.

To test this hypothesis directly, explants were treated with 2 μM CHIR, 50 ng/ml BMP4, or a combination of both. Hair cells were visualized and counted using a POU4F3 antibody to label the nuclei of all hair cells. In explants treated with BMP4 alone, there was no significant change to the number of IHCs or OHCs when compared to DMSO-treated controls (Avg. IHCs in DMSO-treated explants = 370 ± 21. Avg IHCs in BMP4-treated explants = 383 ± 31. Avg. OHCs in DMSO-treated explants = 1055 ± 70. Avg. OHCs in BMP4-treated controls = 1220 ± 74) (Fig. 8F–J). As described, treatment with CHIR alone induced a significant increase in the number of IHCs and a significant decrease in the number of OHCs (Fig. 8H). However, when BMP4 was added to explants also treated with CHIR, there was a significant decrease in the number of IHCs ($p = 0.015$) and an increase in the number of OHCs relative to CHIR treatment alone ($p = 0.007$) (Avg. IHCs in CHIR + BMP4-treated explants = 748 ± 25. Avg. OHCs in CHIR + BMP4-treated explants = 1066 ± 75) (Fig. 8F–J). Treatment with CHIR + BMP4 was sufficient to return the number of OHCs to control values (n.s.); however, IHCs, while significantly reduced relative to CHIR-treatment alone, remained significantly elevated relative to control ($p < 0.0001$). Consistent with the change in hair cell fates, *Fgf10* expression was reduced in explants treated with CHIR and BMP4 relative to those treated with CHIR alone (Fig. 8A, $p = 0.01$). These results indicated that treatment with BMP4 can partially rescue the phenotype observed in response to inhibition of GSK3. The continued increase in IHCs may be a result of a persistent effect of GSK3 inhibition on the medial boundary.

## 3. Discussion

### 3.1. Effects of inhibition of GSK3

The results presented in this study demonstrate an important role for GSK3 in cell fate determination and patterning in the cochlear duct. Inhibition of GSK3 beginning at E13.5 induced an increase in the total number of hair cells and in IHCs in particular, while decreasing the number of OHCs. These results are consistent with changes in two processes during cochlear development, the specification of the size of the prosensory domain and the partitioning of cells within that domain to medial and lateral fates. It is not clear whether these two events occur simultaneously during cochlear development or are temporally separated; however, expression of early markers for the prosensory domain, such as CDKN1β (Chen and Segil, 1999; Lee et al., 2006), and for the lateral prosensory domain, such as PROX1 or *Fgfr3* (Bermingham-McDonogh et al., 2006; Colvin et al., 1996; Mueller et al., 2002), suggests that overall prosensory specification precedes specification of the medial and lateral regions by approximately 24 h. Further, as will be discussed below, fate-mapping studies presented as part of this study indicate that cells within the medial and lateral domains retain some ability to change fates for a limited period of time after the initial specification.

GSK3α and GSK3β are kinases that have been shown to modulate multiple signaling pathways including Wnt, Notch, Hedgehog, and Tgf/Bmp (Patel and Woodgett, 2017). However, previous studies that examined changes in cochlear development following inhibition of GSK3 attributed the effects to activation of the canonical Wnt signaling pathway (Jacques et al., 2012; Munnamalai and Fekete, 2016; Roccio et al., 2015). While activation of Wnt signaling is a common effect of inhibition of GSK3, studies examining the sequestering of signaling molecules to subcellular domains have suggested that Wnt signaling is largely unaffected unless greater than 80% of GSK3 activity is inhibited due to the high affinity and relatively low abundance of AXIN relative to GSK3 (Doble et al., 2007). In other words, the low abundance of AXIN compared to GSK3 means that non-Wnt mediated effects of GSK3 signaling will be inhibited at lower concentrations or GSK3 antagonists (Patel and Woodgett, 2017). Previous studies exposed developing cochlear cultures to a 10 μM concentration of CHIR99021 (Jacques et al., 2012; Munnamalai and Fekete, 2016). At this concentration, significant increases in several known Wnt target genes were observed, and the cellular response included a significant increase in cellular proliferation, a known effect of activation of canonical Wnt. For our experiments, we sought to reveal the non-Wnt-mediated roles of GSK3 by limiting our concentration of CHIR99021 to 2 μM. Expression of Wnt target genes and the level of cellular proliferation were unchanged in 2 μM CHIR-treated explants, suggesting that canonical Wnt signaling was not activated. Moreover, the increase in medial hair cells observed in response to GSK3 inhibition occurred even in the presence of the canonical Wnt antagonist FH535, further supporting the hypothesis that GSK3 modulates hair cell fates through a non-Wnt pathway. However, we cannot rule out the possibility that treatment with CHIR modulates multiple pathways, including canonical Wnt, and that the differences observed in the phenotypes between CHIR-treatment and Wnt-agonist-treatment are a result of multiple pathway influences in the same tissue.

While we did not identify the specific alternate pathways that might be mediating the two observed cochlear phenotypes, there are several possible GSK3-mediated effects that could be involved (Fig. 9). *Bmp4*

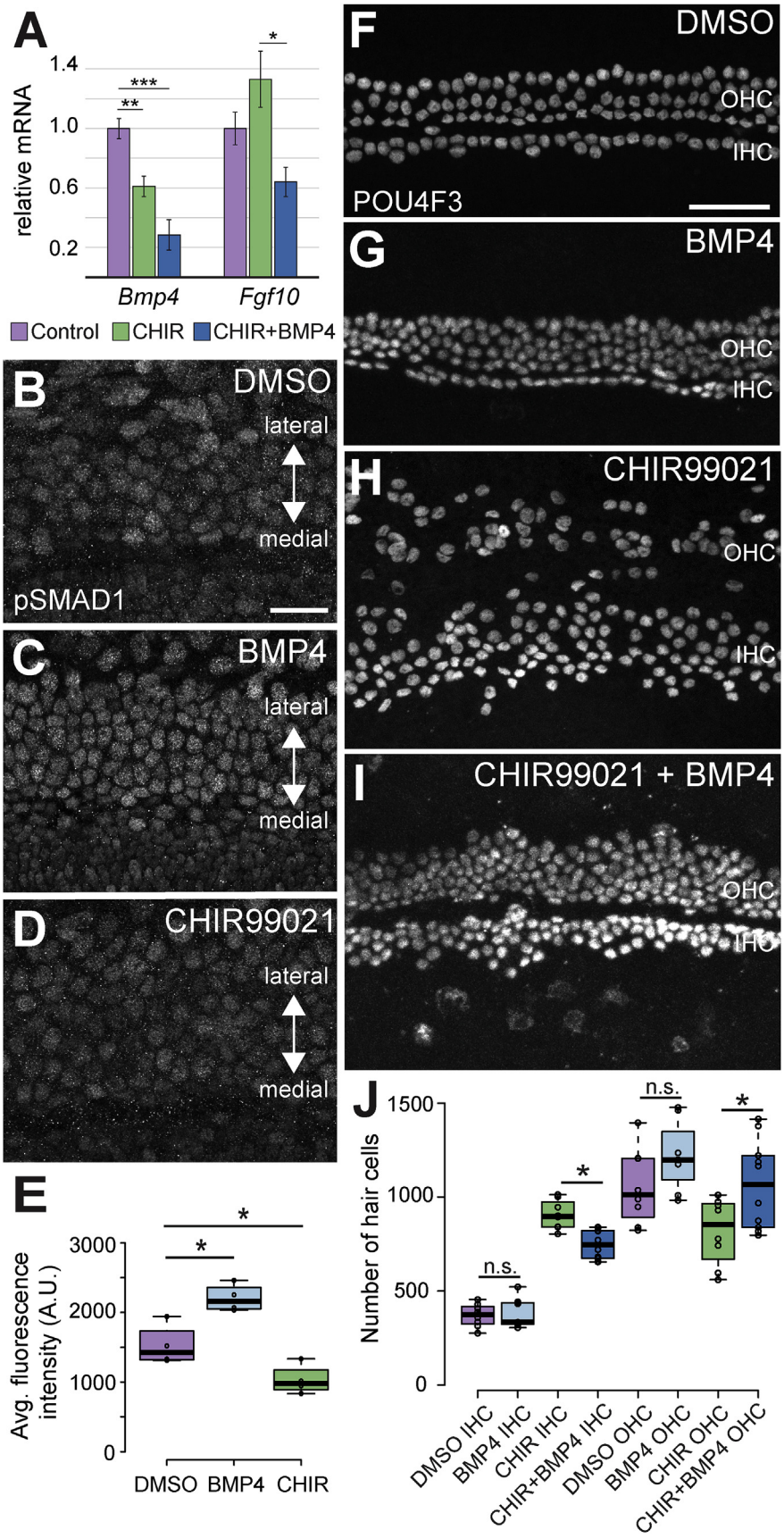


**Fig. 8. The effects of inhibition of GSK3 can be partially rescued by BMP4**

**A.** qRT-PCR quantification of effects of CHIR or CHIR plus BMP4 on expression of *Bmp4* and *Fgf10* in cochlear explants. In CHIR-treated explants, *Bmp4* is significantly decreased ($p = 0.0012$) while levels of *Fgf10* are higher but variable (n.s., $p = 0.22$). In double-treated explants, *Fgf10* is reduced relative to CHIR-treated ($p = 0.012$), but does not differ from controls (n.s., $p = 0.29$). **B-D.** Level of pSMAD1 in the sensory region of explants established on E13.5 and treated with DMSO, BMP4 (50 ng/ml) or CHIR (2 μM) for 4 DIV. Levels of pSMAD1 are higher in response to treatment with BMP4 (C) and lower in explants treated with CHIR (D). **E.** Quantification of average fluorescence intensity for pSMAD1 in cells for each of the three conditions in B-D. pSMAD1 intensity is significantly increased in response to BMP4 and significantly decreased in response to CHIR (N = 4 for each condition. DMSO vs. BMP4 explants, $p = 0.0055$. DMSO vs CHIR explants, $p = 0.030$). **F–I.** Surface views of the middle regions from explants established and maintained as described, stained for POU4F3. Treatment with BMP4 alone does not change the ratio of IHCs to OHCs. CHIR-treatment induces a significant change in the IHC/OHC ratio, but addition of BMP4 results in a partial rescue of the normal phenotype. **J.** Quantification of changes in the number of IHCs and OHCs under the conditions in F–I. Addition of BMP4 significantly reduces the CHIR-mediated increase in IHCs and significantly increases the number of OHCs. While IHCs are still significantly elevated in CHIR + BMP4-treated explants relative to control ($p < 0.0001$), OHCs are not significantly different between CHIR + BMP4 and control ($p = 0.86$). All IHCs comparisons are significant except DMSO vs. BMP4. No OHC comparisons differ except CHIR + BMP4 vs. DMSO or CHIR ($p = 0.0004$, 0.012). DMSO-treated explants N = 11, BMP4-treated explants N = 7. CHIR-treated explants N = 11. CHIR + BMP4 treated explants N = 10. Scale bars (B–D) = 25 μm. Scale bars (F–I) = 50 μm.

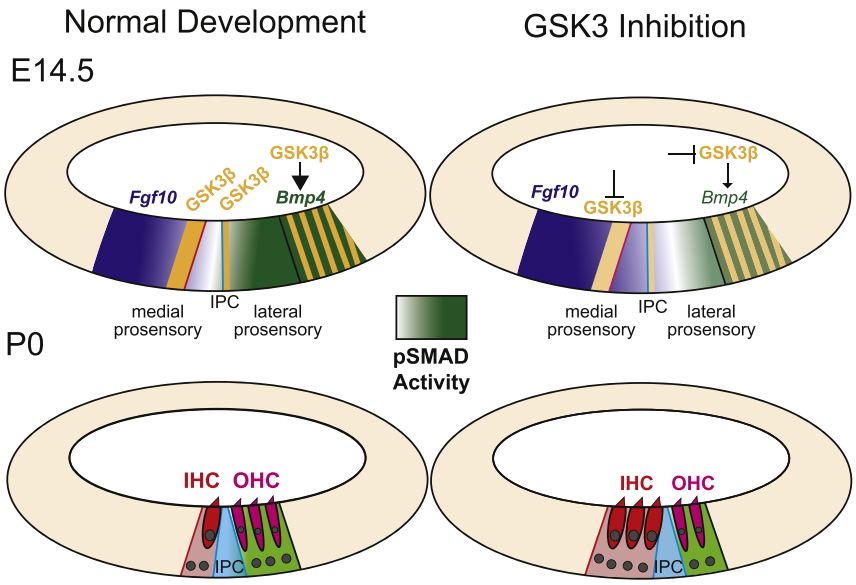


**Fig. 9. Summary of the effects of inhibition of GSK3**
At E14.5 the cochlear duct contains medial and lateral prosensory domains. GSK3β (orange) is expressed at the boundaries between each of the two domains and between the prosensory and non-sensory cells. The boundary between medial and lateral prosensory domains (blue line) aligns with the position of the inner pillar cell (IPC). At the lateral boundary, GSK3β expression overlaps with *Bmp4*. Data presented in this study illustrates that *Bmp4* expression is dependent on GSK3 activity. Expression of *Bmp4* leads to a gradient of pSMAD that extends medially (light green). The level of pSMAD acts to maintain the boundary between the medial and lateral prosensory domains. As a result, at P0, cells within the medial prosensory domain have developed as inner hair cells (red) while cells in the lateral prosensory domain have developed as outer hair cells (magenta). When GSK3 activity is inhibited, two changes occur. *Bmp4* expression decreases, leading to a lateral shift in the gradient of pSMAD. As a result, the lateral prosensory domain is decreased in size, leading to a relative change in the position of the IPC, more IHCs, and fewer OHCs. In addition, the medial boundary between prosensory and non-sensory regions is shifted medially, leading to an additional increase in IHCs. The molecular basis for the medial expansion of the medial prosensory domain is not clear but may be mediated through changes in Notch pathway activity.

expression was decreased in explants treated with CHIR, and the phenotypic switch between IHCs and OHCs was largely rescued by the addition of BMP4. These results suggest that the effects of GSK3β on hair cell phenotype are mediated through BMP4. GSK3 has been shown to inhibit TGFβ (and to a lesser extent BMP) signaling through phosphorylation of SMADs 3 and 4 leading to their degradation through ubiquitination (Demagny et al., 2014; Guo et al., 2008). Since GSK3 is normally active in its base state, inhibition often leads to an increase in expression of TGFβ, which requires both SMAD3 and SMAD4, and BMP4, which requires SMAD1/5/8, through increased activation of existing positive feedback loops (Ohyama et al., 2010). In cochlea, *Bmp4* expression was decreased rather than increased in response to inhibition of GSK3. This result was surprising considering that GSK3β and *Bmp4* are co-expressed in lateral precursor cells. One possible explanation for this result could be related to the strong expression of *Tgfβ2* in the same cells (Pelton et al., 1990; Schmid et al., 1991). Intracellular signaling through both pathways requires the formation of complexes between either SMAD2/3 or SMAD1/5/8 with SMAD4 (Nickel et al., 2018; Wu et al., 2016). Therefore, limited availability of SMAD4 could result in competition between the Tgfβ and Bmp pathways. In this case, inhibition of GSK3 could inhibit degradation of SMAD3, leading to increased activation of Tgfβ signaling and to reduced availability of SMAD4, leading to a decreased activation of the Bmp pathway. Since *Bmp4* expression in the cochlea is dependent on activation of the Bmp signaling pathway (Ohyama et al., 2010), disruption of Bmp intracellular signaling could then lead to a decrease in *Bmp4* expression.

An alternative explanation for the decrease in *Bmp4* expression in response to inhibition of GSK3 could be an indirect effect through another cell type(s), such as the *Fgfr3*$^{+}$ lateral prosensory cells. Deletion of *Fgfr3* leads to an increase in the number of OHCs and in *Bmp4* expression (Puligilla et al., 2007), suggesting that OHCs could stimulate *Bmp4* expression in the adjacent lateral compartment. Inhibition of GSK3 significantly decreases the number of OHCs, which might then decrease the abundance of an undefined inductive signal for *Bmp4*.

In contrast with the phenotypic switch between IHCs and OHCs, the effects of inhibition of GSK3 on the size of the medial domain may be explained through the known interactions between GSK3 and Notch signaling (Espinosa et al., 2003; Han et al., 2012; Jin et al., 2009). Deletion of the Notch ligand *Jagged1* has been shown to lead to a medial shift in the boundary between Kölliker's organ (KO) and the medial edge of the OC, leading to increased rows of IHCs and IPhCs (Brooker et al., 2006; Kiernan et al., 2001). This result suggests that Notch signaling normally acts to set the medial boundary between sensory and non-sensory regions of the duct (Basch et al., 2016b). GSK3 has been shown to phosphorylate NOTCH1, leading to stabilization and increased signaling (Foltz et al., 2002; Kunnimalaiyaan et al., 2015). Therefore, inhibition of GSK3 might increase NOTCH1 degradation leading to decreased notch signaling and a shift in the medial boundary.

### 3.2. Determination of medial and lateral fates

As discussed, the prosensory domain of the cochlea is thought to become separated into medial and lateral domains. Expression of both *Fgfr3* and *Prox1* is initiated in the lateral domain beginning around E13.5 (Bermingham-McDonogh et al., 2006; Fritzsch et al., 2010). Expression data from later time points (Bermingham-McDonogh et al., 2006; Colvin et al., 1996; McGovern et al., 2017; Peters et al., 1993; Pirvola et al., 2002) and fate-mapping using *Fgfr3*$^{icre}$ indicate that cells within the *Fgfr3/Prox1* domain normally give rise to only OHCs, DCs, IPCs, and OPCs (Ellis, Lemons and Kelley, unpublished). Moreover, deletion of *Fgfr3* leads to defects that are restricted, within the ear, to those same cell types (Colvin et al., 1996; Hayashi et al., 2007; Puligilla et al., 2007). However, inhibition of GSK3 led to some *Fgfr3*$^{+}$ cells developing as IHCs and IPhCs, demonstrating that expression of *Fgfr3* does not commit cells to lateral fates. Rather, expression of BMP4 arising from the lateral domain appears to induce or maintain lateral fates in the *Fgfr3/Prox1* domain. Consistent with this hypothesis, deletion of the Bmp antagonist *Noggin* results in extra OHCs in the lateral domain (Hwang et al., 2010). In addition, development of OHCs and the lateral compartment, while somewhat disrupted, is grossly normal in both *Fgfr3* and *Prox1* mutants (Colvin et al., 1996; Fritzsch et al., 2010; Hayashi et al., 2007; Kirjavainen et al., 2008; Puligilla et al., 2007). As a secreted molecule, BMP4 is presumably acting in a paracrine fashion to specify lateral fates; however, other unidentified factors must also be acting to create the precise boundaries observed at both the pillar and Hensen's borders of the OHC/lateral domain. Finally, while expression of *Fgfr3/Prox1* does not, apparently, restrict cell fates, the precision of the boundaries of this domain, as well as the adjacent *Bmp4* domain, strongly suggest that additional patterning signals must be working prior to the onset of expression of *Fgfr3/Prox1/Bmp4* to precisely define specific boundaries

within the cochlear duct. The identification of these factors would provide valuable insights regarding overall patterning within the cochlear duct and the mechanisms that lead to the formation of OHCs and DCs, which could be essential for the development of regenerative strategies for these unique cell types.

### 3.3. Specification of the medial-lateral axis of the cochlear duct

As discussed, the OC is asymmetricly patterned along its medial-lateral axis. However, axial patterning clearly extends along the full extent of the medial-lateral axis as non-sensory cells located either medial (KO) or lateral (outer sulcus) to the OC show distinct morphological and transcriptional characteristics throughout development. The factors that specify regional identities across this axis remain poorly understood. *Bmp4* and *Fgf10* are localized, respectively, to the lateral and medial regions of the duct as early as E12.5, well before terminal mitosis or any obvious cellular commitment (Ohyama et al., 2010; Urness et al., 2015; Wright and Mansour, 2003). Partial deletion of the Bmp4 receptors *Alk3* and *Alk6* leads to an increase in expression of *Fgf10* along with a general disruption in medial-lateral patterning (Ohyama et al., 2010). These results, along with previous studies demonstrating cross-regulatory interactions between Bmps and Fgfs (Fritzsch et al., 2006), led to the suggestion that counter gradients of *Bmp4* and *Fgf10* might regulate regional cochlear identities, and while we observe a decrease in *Bmp4* expression in response to inhibition of GSK3, we did not observe a statistically significant increase in expression of *Fgf10*. Since CHIR was not added to cochlear explants until E13.5, it is possible that a critical period for regulation of *Fgf10* by *Bmp4* had ended. Alternatively, deletion of *Fgf10* has recently been shown to not alter cellular patterning along the cochlear medial-lateral axis (Urness et al., 2015), suggesting that other factors must play significant roles in the specification of identities along this axis.

## 4. Materials and methods

Mouse strains – Timed pregnant CD1 mice were obtained from Charles River Laboratories. *Fgfr3*$^{icreERT2}$ (Stock no. 025809), *Atoh1*$^{tm4.1Hzo}$ (Stock no. 013593) and tdTomato*Gt(ROSA)26 Sor*$^{tm14(CAG-tdTomato)Hze}$ Stock no. 007914) were all obtained from Jackson Laboratories. Fgf8$^{GFP}$ mice were obtained from Anne Moon.

Cochlear explants – Embryos were dissected from timed pregnant CD1 female mice at embryonic day 13.5 or 14.5, as indicated. Cochleae were dissected and plated on MatTek dishes coated with 7% Matrigel (BD Biosciences Cat. No. 354234) in DMEM as described (Driver and Kelley, 2010). Cochleae were cultured with phenol red free DMEM containing 10% FBS and 1 μg/mL ciprofloxin at 37 °C. Culture media containing pharmacological inhibitors was changed every day.

Pharmacological inhibitors – CHIR9901 (CAS# 252917-06-9. Tocris Bioscience. Cat. No. 4423) was resuspended in DMSO at a stock concentration of 1 mM and used at a concentration of 2 μM. BIO-acetoxime (CAS# 667463-85-6. Tocris Bioscience. Cat. No. 3874) was resuspended in DMSO at a stock concentration of 20 mM and used at a concentration of 1 μM. WntAgonist (CAS# 853220-52-7. Calbiochem. Cat. No. 681665) was resuspended in DMSO at a concentration of 20 mM and used at a concentration of 250 nM. SU 5402 (CAS# 215543-92-3. Tocris Bioscience. Cat. No. 3300) was resuspended in DMSO at a concentration of 10 mM and used at a concentration of 10 μM. Culture media containing pharmacological inhibitors was changed every day.

Recombinant protein – Recombinant Mouse BMP4 (R&D Systems. Cat. No. 5020-BP-010) was reconstituted at 100 μg/mL in sterile 4 mM HCl with 0.1% BSA and used on explants at a concentration of 50 ng/mL.

EdU proliferation assay – Cell proliferation was detected using the Click-iT EdU Imaging Kits. (ThermoFisher Scientific. Cat.No. C10340) per the manufacturers protocol.

Immunohistochemistry – Explants were fixed with 4% PFA at room temperature for 20 min. Explants were washed with PBS and then blocked with PBS containing 10% Normal Horse Serum (Jackson ImmunoResearch Labs. Cat. No. 008-000-121) and 0.1% TritonX100 for 20 min at room temperature. Explants were incubated in primary antibody overnight at 4 °C. Primary antibodies used: Rabbit anti-GSK3β at 1:250 (Abcam. Cat. No. ab32391), Rabbit anti-GSK3β at 1:500 (Cell Signaling Technology. Cat. No. 12456), Rabbit anti-MYOSIN7A or MYOSIN6 at 1:1000 (Proteus Biosciences Inc. Cat. Nos. 25–6790, 25–6791), Mouse anti-MYOSIN7A at 1:200 (Developmental Studies Hybridoma Bank. Cat. No. MYO7A 138–1), Chicken anti-GFP at 1:1000 (AvesLab. Cat. No. GFP-1020), first blocked with BlokhenII according to manufacturer's protocol (AvesLab. Cat.No. BH-1001), Sheep anti-S100A1 at 1:200 (R&D Systems. Cat. No. AF4138), Sheep anti-CDH2 at 1:500 (R&D Systems. Cat. No. AF6426), Mouse anti-CALB1 at 1:500 (Abcam Cat. No. 82812), Goat anti-NGFR at 1:500 (R&D Systems. Cat. No. AF367), Goat anti-SOX2 at 1:500 (Santa Cruz Biotechnology. Cat. No. sc-17320), Rabbit anti-PROX1 at 1:500 (Millipore. Cat. No. AB5475), Rabbit anti-DSRED at 1:500 (Clontech. Cat. No. 632496), Rabbit anti-pSMAD1 (Ser 463/465) at 1:100 with MeOH permeabilization according to manufacturer's protocol (Cell Signaling Technology. Cat. No. 9516), Mouse anti-POU4F3 (formerly Brn3-c) at 1:200 (Santa Cruz Biotechnology. Cat. No. sc-81980), and Phalloidin Alexa Fluor 647 at 1:500 (ThermoFisher Scientific. Cat. No. A22287). Secondary antibodies were used at 1:1000: Donkey anti-Rabbit Alexa Fluor 555 (ThermoFisher Scientific. Cat. No. A-31572), Donkey anti-Goat Alexa Fluor 488, 647 (ThermoFisher Scientific. Cat. No. A-11055, Cat. No. A-21447), Donkey anti-Mouse Alexa Fluor 488, 647 (ThermoFisher Scientific. Cat. No. A-21202, Cat. No. A-31571), and Donkey anti-Chicken Alexa Fluor 488 (Jackson ImmunoResearch Labs. Cat. No. 703-545-155).

qRT-PCR – mRNA was extracted from explants using Arcturus PicoPure RNA Isolation Kit (ThermoFisher Scientific. Cat. No. KIT0204) per manufacturer's protocol. cDNA was generated using SuperScript IV First-Strand Synthesis System (ThermoFisher Scientific. Cat. No. 18091050) per manufacturer's protocol. qPCR was performed using TaqMan Fast Advanced Master Mix (Applied Biosystems. ThermoFisher. Cat. No. 4444557) using the following TaqMan probes (ThermoFisher. Cat. No. 4331182): *Gapdh* (Mm99999915_g1), *Fgf10* (Mm00433275_m1), *Bmp4* (Mm00432087_m1), *Lgr5* (Mm00438890_m1), *Axin2* (Mm00443610_m1), and *Ccnd1* (Mm00432359_m1).

### 4.1. Statistical analysis

Statistical comparisons were conducted using GraphPad Prism. Student's unpaired, two-tailed *t*-test was used for comparing two values. For multiple comparisons, ordinary one-way ANOVA was followed by Dunnett's multiple comparisons test or Tukey's multiple comparisons test as appropriate.

## Acknowledgements

The authors would like to thank the animal care and use staff at the Shared Animal Facility, Porter Neuroscience Building for outstanding animal care. We would also like to thank Drs. Lisa Cunningham and Katie Kindt for reading an earlier version of the manuscript. This research was supported by the Intramural Research Program of the NIDCD, NIH (DC000059 to M.W.K.).

## Appendix A. Supplementary data

Supplementary data to this article can be found online at https://doi.org/10.1016/j.ydbio.2019.06.003.

## References

Basch, M.L., Brown 2nd, R.M., Jen, H.I., Groves, A.K., 2016a. Where hearing starts: the development of the mammalian cochlea. J. Anat. 228, 233–254.
Basch, M.L., Brown 2nd, R.M., Jen, H.I., Semerci, F., Depreux, F., Edlund, R.K., Zhang, H., Norton, C.R., Gridley, T., Cole, S.E., Doetzlhofer, A., Maletic-Savatic, M., Segil, N.,

Groves, A.K., 2016b. Fine-tuning of Notch signaling sets the boundary of the organ of Corti and establishes sensory cell fates. Elife 5.
Bennett, C.N., Ross, S.E., Longo, K.A., Bajnok, L., Hemati, N., Johnson, K.W., Harrison, S.D., MacDougald, O.A., 2002. Regulation of Wnt signaling during adipogenesis. J. Biol. Chem. 277, 30998–31004.
Bermingham-McDonogh, O., Oesterle, E.C., Stone, J.S., Hume, C.R., Huynh, H.M., Hayashi, T., 2006. Expression of Prox1 during mouse cochlear development. J. Comp. Neurol. 496, 172–186.
Bermingham, N.A., Hassan, B.A., Price, S.D., Vollrath, M.A., Ben-Arie, N., Eatock, R.A., Bellen, H.J., Lysakowski, A., Zoghbi, H.Y., 1999. Math1: an essential gene for the generation of inner ear hair cells. Science 284, 1837–1841.
Brooker, R., Hozumi, K., Lewis, J., 2006. Notch ligands with contrasting functions: Jagged1 and Delta 1 in the mouse inner ear. Development 133, 1277–1286.
Chacon-Heszele, M.F., Ren, D., Reynolds, A.B., Chi, F., Chen, P., 2012. Regulation of cochlear convergent extension by the vertebrate planar cell polarity pathway is dependent on p120-catenin. Development 139, 968–978.
Chen, P., Segil, N., 1999. p27(Kip 1) links cell proliferation to morphogenesis in the developing organ of Corti. Development 126, 1581–1590.
Colvin, J.S., Bohne, B.A., Harding, G.W., McEwen, D.G., Ornitz, D.M., 1996. Skeletal overgrowth and deafness in mice lacking fibroblast growth factor receptor 3. Nat. Genet. 12, 390–397.
Coppens, A.G., Kiss, R., Heizmann, C.W., Schafer, B.W., Poncelet, L., 2001. Immunolocalization of the calcium binding S100A1, S100A5 and S100A6 proteins in the dog cochlea during postnatal development. Brain Res Dev Brain Res 126, 191–199.
Dabdoub, A., Puligilla, C., Jones, J.M., Fritzsch, B., Cheah, K.S., Pevny, L.H., Kelley, M.W., 2008. Sox2 signaling in prosensory domain specification and subsequent hair cell differentiation in the developing cochlea. Proc. Natl. Acad. Sci. U. S. A. 105, 18396–18401.
Dechesne, C.J., Thomasset, M., 1988. Calbindin (CaBP 28 kDa) appearance and distribution during development of the mouse inner ear. Brain Res. 468, 233–242.
Demagny, H., Araki, T., De Robertis, E.M., 2014. The tumor suppressor Smad4/DPC4 is regulated by phosphorylations that integrate FGF, Wnt, and TGF-beta signaling. Cell Rep. 9, 688–700.
Deng, M., Luo, X.J., Pan, L., Yang, H., Xie, X., Liang, G., Huang, L., Hu, F., Kiernan, A.E., Gan, L., 2014. LMO4 functions as a negative regulator of sensory organ formation in the mammalian cochlea. J. Neurosci. 34, 10072–10077.
Doble, B.W., Patel, S., Wood, G.A., Kockeritz, L.K., Woodgett, J.R., 2007. Functional redundancy of GSK-3alpha and GSK-3beta in Wnt/beta-catenin signaling shown by using an allelic series of embryonic stem cell lines. Dev. Cell 12, 957–971.
Driver, E.C., Kelley, M.W., 2009. Specification of cell fate in the mammalian cochlea. Birth Defects Res. Part C Embryo Today - Rev. 87, 212–221.
Driver, E.C., Kelley, M.W., 2010. Transfection of mouse cochlear explants by electroporation. Current protocols in neuroscience 51 (Chapter 4), 4.34.1-10.
Driver, E.C., Northrop, A., Kelley, M.W., 2017. Cell migration, intercalation and growth regulate mammalian cochlear extension. Development 144, 3766–3776.
Driver, E.C., Pryor, S.P., Hill, P., Turner, J., Ruther, U., Biesecker, L.G., Griffith, A.J., Kelley, M.W., 2008. Hedgehog signaling regulates sensory cell formation and auditory function in mice and humans. J. Neurosci. 28, 7350–7358.
Espinosa, L., Ingles-Esteve, J., Aguilera, C., Bigas, A., 2003. Phosphorylation by glycogen synthase kinase-3 beta down-regulates Notch activity, a link for Notch and Wnt pathways. J. Biol. Chem. 278, 32227–32235.
Foltz, D.R., Santiago, M.C., Berechid, B.E., Nye, J.S., 2002. Glycogen synthase kinase-3beta modulates notch signaling and stability. Curr. Biol. 12, 1006–1011.
Fritzsch, B., Beisel, K.W., Hansen, L.A., 2006. The molecular basis of neurosensory cell formation in ear development: a blueprint for hair cell and sensory neuron regeneration? Bioessays 28, 1181–1193.
Fritzsch, B., Dillard, M., Lavado, A., Harvey, N.L., Jahan, I., 2010. Canal cristae growth and fiber extension to the outer hair cells of the mouse ear require Prox1 activity. PLoS One 5, e9377.
Fuentealba, L.C., Eivers, E., Ikeda, A., Hurtado, C., Kuroda, H., Pera, E.M., De Robertis, E.M., 2007. Integrating patterning signals: Wnt/GSK3 regulates the duration of the BMP/Smad1 signal. Cell 131, 980–993.
Groves, A.K., Fekete, D.M., 2012. Shaping sound in space: the regulation of inner ear patterning. Development 139, 245–257.
Gu, R., Brown 2nd, R.M., Hsu, C.W., Cai, T., Crowder, A.L., Piazza, V.G., Vadakkan, T.J., Dickinson, M.E., Groves, A.K., 2016. Lineage tracing of Sox2-expressing progenitor cells in the mouse inner ear reveals a broad contribution to non-sensory tissues and insights into the origin of the organ of Corti. Dev. Biol. 414, 72–84.
Guo, X., Ramirez, A., Waddell, D.S., Li, Z., Liu, X., Wang, X.F., 2008. Axin and GSK3-control Smad3 protein stability and modulate TGF- signaling. Genes Dev. 22, 106–120.
Han, H., Tanigaki, K., Yamamoto, N., Kuroda, K., Yoshimoto, M., Nakahata, T., Ikuta, K., Honjo, T., 2002. Inducible gene knockout of transcription factor recombination signal binding protein-J reveals its essential role in T versus B lineage decision. Int. Immunol. 14, 637–645.
Han, X., Ju, J.H., Shin, I., 2012. Glycogen synthase kinase 3-beta phosphorylates novel S/T-P-S/T domains in Notch1 intracellular domain and induces its nuclear localization. Biochem. Biophys. Res. Commun. 423, 282–288.
Handeli, S., Simon, J.A., 2008. A small-molecule inhibitor of Tcf/beta-catenin signaling down-regulates PPARgamma and PPARdelta activities. Mol. Cancer Ther. 7, 521–529.
Hartman, B.H., Reh, T.A., Bermingham-McDonogh, O., 2010. Notch signaling specifies prosensory domains via lateral induction in the developing mammalian inner ear. Proc. Natl. Acad. Sci. U. S. A. 107, 15792–15797.
Hayashi, T., Cunningham, D., Bermingham-McDonogh, O., 2007. Loss of Fgfr3 leads to excess hair cell development in the mouse organ of Corti. Dev. Dynam. 236, 525–533.
Hayashi, T., Ray, C.A., Bermingham-McDonogh, O., 2008. Fgf20 is required for sensory epithelial specification in the developing cochlea. J. Neurosci. 28, 5991–5999.
Hoeflich, K.P., Luo, J., Rubie, E.A., Tsao, M.S., Jin, O., Woodgett, J.R., 2000. Requirement for glycogen synthase kinase-3beta in cell survival and NF-kappaB activation. Nature 406, 86–90.
Hwang, C.H., Guo, D., Harris, M.A., Howard, O., Mishina, Y., Gan, L., Harris, S.E., Wu, D.K., 2010. Role of bone morphogenetic proteins on cochlear hair cell formation: analyses of Noggin and Bmp2 mutant mice. Dev. Dynam. 239, 505–513.
Jacques, B.E., Montcouquiol, M.E., Layman, E.M., Lewandoski, M., Kelley, M.W., 2007. Fgf8 induces pillar cell fate and regulates cellular patterning in the mammalian cochlea. Development 134, 3021–3029.
Jacques, B.E., Montgomery, W.H.t., Uribe, P.M., Yatteau, A., Asuncion, J.D., Resendiz, G., Matsui, J.I., Dabdoub, A., 2014. The role of Wnt/beta-catenin signaling in proliferation and regeneration of the developing basilar papilla and lateral line. Dev Neurobiol 74, 438–456.
Jacques, B.E., Puligilla, C., Weichert, R.M., Ferrer-Vaquer, A., Hadjantonakis, A.-K., Kelley, M.W., Dabdoub, A., 2012. A dual function for canonical Wnt/β-catenin signaling in the developing mammalian cochlea. Development 139, 4395–4404.
Jin, Y.H., Kim, H., Oh, M., Ki, H., Kim, K., 2009. Regulation of Notch1/NICD and Hes1 expressions by GSK-3alpha/beta. Mol. Cells 27, 15–19.
Kelley, M.W., Driver, E.C., Puligilla, C., 2009. Regulation of cell fate and patterning in the developing mammalian cochlea. Curr. Opin. Otolaryngol. Head Neck Surg. 17, 381–387.
Kerkela, R., Kockeritz, L., Macaulay, K., Zhou, J., Doble, B.W., Beahm, C., Greytak, S., Woulfe, K., Trivedi, C.M., Woodgett, J.R., Epstein, J.A., Force, T., Huggins, G.S., 2008. Deletion of GSK-3beta in mice leads to hypertrophic cardiomyopathy secondary to cardiomyoblast hyperproliferation. J. Clin. Investig. 118, 3609–3618.
Kiernan, A.E., Ahituv, N., Fuchs, H., Balling, R., Avraham, K.B., Steel, K.P., Hrabe de Angelis, M., 2001. The Notch ligand Jagged1 is required for inner ear sensory development. Proc. Natl. Acad. Sci. U. S. A. 98, 3873–3878.
Kiernan, A.E., Cordes, R., Kopan, R., Gossler, A., Gridley, T., 2005a. The Notch ligands DLL1 and JAG2 act synergistically to regulate hair cell development in the mammalian inner ear. Development 132, 4353–4362.
Kiernan, A.E., Pelling, A.L., Leung, K.K., Tang, A.S., Bell, D.M., Tease, C., Lovell-Badge, R., Steel, K.P., Cheah, K.S., 2005b. Sox2 is required for sensory organ development in the mammalian inner ear. Nature 434, 1031–1035.
Kim, W.Y., Wang, X., Wu, Y., Doble, B.W., Patel, S., Woodgett, J.R., Snider, W.D., 2009. GSK-3 is a master regulator of neural progenitor homeostasis. Nat. Neurosci. 12, 1390–1397.
Kirjavainen, A., Sulg, M., Heyd, F., Alitalo, K., Yla-Herttuala, S., Moroy, T., Petrova, T.V., Pirvola, U., 2008. Prox1 interacts with Atoh1 and Gfi1, and regulates cellular differentiation in the inner ear sensory epithelia. Dev. Biol. 322, 33–45.
Kramer, T., Schmidt, B., Lo Monte, F., 2012. Small-molecule inhibitors of GSK-3: structural insights and their application to alzheimer's disease models. Int. J. Alzheimer's Dis. 2012, 381029.
Kunnimalaiyaan, S., Gamblin, T.C., Kunnimalaiyaan, M., 2015. Glycogen synthase kinase-3 inhibitor AR-A014418 suppresses pancreatic cancer cell growth via inhibition of GSK-3-mediated Notch1 expression. HPB 17, 770–776.
Larner, J., Villar-Palasi, C., Goldberg, N.D., Bishop, J.S., Huijing, F., Wenger, J.I., Sasko, H., Brown, N.B., 1968. Hormonal and non-hormonal control of glycogen synthesis-control of transferase phosphatase and transferase I kinase. Adv. Enzym. Regul. 6, 409–423.
Lee, Y.S., Liu, F., Segil, N., 2006. A morphogenetic wave of p27Kip 1 transcription directs cell cycle exit during organ of Corti development. Development 133, 2817–2826.
Liu, J., Li, G., Liu, D., Liu, J., 2014. FH535 inhibits the proliferation of HepG2 cells via downregulation of the Wnt/beta-catenin signaling pathway. Mol. Med. Rep. 9, 1289–1292.
Liu, J., Wu, X., Mitchell, B., Kintner, C., Ding, S., Schultz, P.G., 2005. A small-molecule agonist of the Wnt signaling pathway. Angew Chem. Int. Ed. Engl. 44, 1987–1990.
MacAulay, K., Doble, B.W., Patel, S., Hansotia, T., Sinclair, E.M., Drucker, D.J., Nagy, A., Woodgett, J.R., 2007. Glycogen synthase kinase 3alpha-specific regulation of murine hepatic glycogen metabolism. Cell Metabol. 6, 329–337.
Mansour, S.L., Twigg, S.R., Freeland, R.M., Wall, S.A., Li, C., Wilkie, A.O., 2009. Hearing loss in a mouse model of Muenke syndrome. Hum. Mol. Genet. 18, 43–50.
McGovern, M.M., Brancheck, J., Grant, A.C., Graves, K.A., Cox, B.C., 2017. Quantitative analysis of supporting cell subtype labeling among CreER lines in the neonatal mouse cochlea. J Assoc Res Otolaryngol 18, 227–245.
Meijer, L., Skaltsounis, A.L., Magiatis, P., Polychronopoulos, P., Knockaert, M., Leost, M., Ryan, X.P., Vonica, C.A., Brivanlou, A., Dajani, R., Crovace, C., Tarricone, C., Musacchio, A., Roe, S.M., Pearl, L., Greengard, P., 2003. GSK-3-selective inhibitors derived from Tyrian purple indirubins. Chem. Biol. 10, 1255–1266.
Miyashita, K., Kawakami, K., Nakada, M., Mai, W., Shakoori, A., Fujisawa, H., Hayashi, Y., Hamada, J., Minamoto, T., 2009. Potential therapeutic effect of glycogen synthase kinase 3beta inhibition against human glioblastoma. Clin. Cancer Res. 15, 887–897.
Morsli, H., Choo, D., Ryan, A., Johnson, R., Wu, D.K., 1998. Development of the mouse inner ear and origin of its sensory organs. J. Neurosci. 18, 3327–3335.
Mueller, K.L., Jacques, B.E., Kelley, M.W., 2002. Fibroblast growth factor signaling regulates pillar cell development in the organ of corti. J. Neurosci. 22, 9368–9377.
Munnamalai, V., Fekete, D.M., 2016. Notch-Wnt-Bmp crosstalk regulates radial patterning in the mouse cochlea in a spatiotemporal manner. Development 143, 4003–4015.
Naujok, O., Lentes, J., Diekmann, U., Davenport, C., Lenzen, S., 2014. Cytotoxicity and activation of the Wnt/beta-catenin pathway in mouse embryonic stem cells treated with four GSK3 inhibitors. BMC Res. Notes 7, 273.

Nickel, J., Ten Dijke, P., Mueller, T.D., 2018. TGF-beta family co-receptor function and signaling. Acta Biochim. Biophys. Sin. 50, 12–36.
Ohyama, T., Basch, M.L., Mishina, Y., Lyons, K.M., Segil, N., Groves, A.K., 2010. BMP signaling is necessary for patterning the sensory and nonsensory regions of the developing mammalian cochlea. J. Neurosci. 30, 15044–15051.
Pan, N., Jahan, I., Kersigo, J., Duncan, J.S., Kopecky, B., Fritzsch, B., 2012. A novel Atoh1 "self-terminating" mouse model reveals the necessity of proper Atoh1 level and duration for hair cell differentiation and viability. PLoS One 7 e30358.
Patel, P., Woodgett, J.R., 2017. Glycogen synthase kinase 3: a kinase for all pathways? Curr. Top. Dev. Biol. 123, 277–302.
Patel, S., Macaulay, K., Woodgett, J.R., 2011. Tissue-specific analysis of glycogen synthase kinase-3alpha (GSK-3alpha) in glucose metabolism: effect of strain variation. PLoS One 6 e15845.
Pauley, S., Wright, T.J., Pirvola, U., Ornitz, D., Beisel, K., Fritzsch, B., 2003. Expression and function of FGF10 in mammalian inner ear development. Dev. Dynam. 227, 203–215.
Pelton, R.W., Dickinson, M.E., Moses, H.L., Hogan, B.L., 1990. In situ hybridization analysis of TGF beta 3 RNA expression during mouse development: comparative studies with TGF beta 1 and beta 2. Development 110, 609–620.
Peters, K., Ornitz, D., Werner, S., Williams, L., 1993. Unique expression pattern of the FGF receptor 3 gene during mouse organogenesis. Dev. Biol. 155, 423–430.
Pirvola, U., Ylikoski, J., Trokovic, R., Hebert, J.M., McConnell, S.K., Partanen, J., 2002. FGFR1 is required for the development of the auditory sensory epithelium. Neuron 35, 671–680.
Price, M.A., Kalderon, D., 2002. Proteolysis of the Hedgehog signaling effector cubitus interruptus requires phosphorylation by glycogen synthase kinase 3 and casein kinase 1. Cell 108, 823–835.
Puligilla, C., Feng, F., Ishikawa, K., Bertuzzi, S., Dabdoub, A., Griffith, A.J., Fritzsch, B., Kelley, M.W., 2007. Disruption of fibroblast growth factor receptor 3 signaling results in defects in cellular differentiation, neuronal patterning, and hearing impairment. Dev. Dynam. 236, 1905–1917.
Ring, D.B., Johnson, K.W., Henriksen, E.J., Nuss, J.M., Goff, D., Kinnick, T.R., Ma, S.T., Reeder, J.W., Samuels, I., Slabiak, T., Wagman, A.S., Hammond, M.E., Harrison, S.D., 2003. Selective glycogen synthase kinase 3 inhibitors potentiate insulin activation of glucose transport and utilization in vitro and in vivo. Diabetes 52, 588–595.
Roccio, M., Hahnewald, S., Perny, M., Senn, P., 2015. Cell cycle reactivation of cochlear progenitor cells in neonatal FUCCI mice by a GSK3 small molecule inhibitor. Sci. Rep. 5, 17886.
Ruben, R.J., 1967. Development of the inner ear of the mouse: a radioautographic study of terminal mitoses. Acta Otolaryngol. Suppl 220, 221–244.
Rubinfeld, B., Albert, I., Porfiri, E., Fiol, C., Munemitsu, S., Polakis, P., 1996. Binding of GSK3beta to the APC-beta-catenin complex and regulation of complex assembly. Science 272, 1023–1026.
Schmid, P., Cox, D., Bilbe, G., Maier, R., McMaster, G.K., 1991. Differential expression of TGF beta 1, beta 2 and beta 3 genes during mouse embryogenesis. Development 111, 117–130.
Shi, F., Hu, L., Jacques, B.E., Mulvaney, J.F., Dabdoub, A., Edge, A.S., 2014. beta-Catenin is required for hair-cell differentiation in the cochlea. J. Neurosci. 34, 6470–6479.
Shim, K., Minowada, G., Coling, D.E., Martin, G.R., 2005. Sprouty2, a mouse deafness gene, regulates cell fate decisions in the auditory sensory epithelium by antagonizing FGF signaling. Dev. Cell 8, 553–564.
Spokoini, R., Kfir-Erenfeld, S., Yefenof, E., Sionov, R.V., 2010. Glycogen synthase kinase-3 plays a central role in mediating glucocorticoid-induced apoptosis. Mol. Endocrinol. 24, 1136–1150.
Stambolic, V., Ruel, L., Woodgett, J.R., 1996. Lithium inhibits glycogen synthase kinase-3 activity and mimics wingless signalling in intact cells. Curr. Biol. 6, 1664–1668.
Tempe, D., Casas, M., Karaz, S., Blanchet-Tournier, M.F., Concordet, J.P., 2006. Multisite protein kinase A and glycogen synthase kinase 3beta phosphorylation leads to Gli3 ubiquitination by SCFbetaTrCP. Mol. Cell. Biol. 26, 4316–4326.
Urness, L.D., Wang, X., Shibata, S., Ohyama, T., Mansour, S.L., 2015. Fgf10 is required for specification of non-sensory regions of the cochlear epithelium. Dev. Biol. 400, 59–71.
Wang, Y., Yang, Z., Meng, Z., Cao, H., Zhu, G., Liu, T., Wang, X., 2013. Knockdown of TRPM8 suppresses cancer malignancy and enhances epirubicin-induced apoptosis in human osteosarcoma cells. Int. J. Biol. Sci. 10, 90–102.
Woods, C., Montcouquiol, M., Kelley, M.W., 2004. Math1 regulates development of the sensory epithelium in the mammalian cochlea. Nat. Neurosci. 7, 1310–1318.
Wright, T.J., Mansour, S.L., 2003. Fgf3 and Fgf10 are required for mouse otic placode induction. Development 130, 3379–3390.
Wu, M., Chen, G., Li, Y.P., 2016. TGF-beta and BMP signaling in osteoblast, skeletal development, and bone formation, homeostasis and disease. Bone Res 4, 16009.
Yost, C., Torres, M., Miller, J.R., Huang, E., Kimelman, D., Moon, R.T., 1996. The axis-inducing activity, stability, and subcellular distribution of beta-catenin is regulated in Xenopus embryos by glycogen synthase kinase 3. Genes Dev. 10, 1443–1454.
Zhang, K.D., Coate, T.M., 2017. Recent advances in the development and function of type II spiral ganglion neurons in the mammalian inner ear. Semin. Cell Dev. Biol. 65, 80–87.
Zheng, J.L., Gao, W.Q., 2000. Overexpression of Math1 induces robust production of extra hair cells in postnatal rat inner ears. Nat. Neurosci. 3, 580–586.